Article

Volatile Compounds from Waste Shiitake Fungi Beds Enhance Rice Growth, Yield, and Performance Under High-Temperature Field Conditions

Clever Nkhokwe Kanga , Rio Umezawa , Setu Rani Saha , Hideyuki Takahashi , Masanori Yamasaki ,
Kimiko Itoh *

Posted Date: 9 April 2026

doi: 10.20944/preprints202604.0584.v1

Keywords: rice(*Oryza sativa*) ; heat stress; plant biostimulant; cytokinin signaling; agroecology; sustainable agriculture; phenological shift; circular bioeconom doi:10.20944/preprints202604.0584.v1

Article

Volatile Compounds from Waste Shiitake Fungi Beds Enhance Rice Growth, Yield, and Performance Under High-Temperature Field Conditions

Clever Nkhokwe Kanga [1], Rio Umezawa [2], Setu Rani Saha [3], Hideyuki Takahashi [4], Masanori Yamasaki [1] and Kimiko Itoh [1,*]

[1] Institute of Science and Technology, Niigata University, Niigata 950-2181, Japan
[2] Graduate School of science and Technology, Niigata University, Niigata 950-2181, Japan
[3] Department of Genetics and Plant Breeding, Bangladesh Agricultural University, Mymensingh-2202, Bangladesh
[4] Department of Agriculture, School of Agriculture, Tokai University, Kumamoto 862-8652, Japan
* Correspondence: kimi@agr.niigata-u.ac.jp; Tel.: +81 252-627-522

Abstract

Agricultural waste streams represent an underutilized source of bioactive compounds with potential to enhance crop resilience under climate stress. We previously showed that volatile compounds (VCs) emitted from waste shiitake fungi beds (WSFBs) promote early rice seedling growth under controlled conditions. Here, we evaluated whether these early-stage effects persist after transplanting and translate into agronomic benefits under field conditions, including during the record high temperatures (HT) of the 2023 growing season in Niigata, Japan. Seedlings of two japonica cultivars, Nipponbare and Koshihikari, were exposed to WSFB-derived VCs using a non-contact system and subsequently grown in paddy fields across two seasons (2023-2024). WSFBs-VC-treated (+VCs) plants exhibited enhanced seedling vigor, advanced heading by 5-6 days under HT conditions, increased tiller and panicle numbers, higher grain yield per plant, greater 1000-grain weight, and reduced grain chalkiness. Gas-exchange measurements at the reproductive stage showed that +VCs plants maintained higher net photosynthetic rate, stomatal conductance, intercellular CO_2 concentration, and transpiration rate, while intrinsic water-use efficiency showed a modest decline consistent with transpirational cooling. Controlled-environment assays further revealed improved physiological stability and upregulation of cytokinin and stress-responsive genes under acute heat stress. Together, these results demonstrate that short-term exposure to WSFBs-derived VCs enhances rice performance under field conditions, including during extreme heat, and highlight the potential of waste-derived fungal volatiles as sustainable biostimulants for climate-resilient rice production.

Keywords: rice(*Oryza sativa*) ; heat stress; plant biostimulant; cytokinin signaling; agroecology; sustainable agriculture; phenological shift; circular bioeconomy

---

1. Introduction

Global population growth and escalating climate change impacts present critical challenges to agriculture, necessitating the development of sustainable food production systems to secure future food supplies [1–3]. Current traditional farming practices are unable to maintain crop productivity under rising environmental stresses [4–6], highlighting the urgent need for novel, sustainable food production technologies. Among these, plant biostimulants (PBs) increase growth, nutrient uptake, and abiotic stress tolerance [7,8], offer promising solutions that align with sustainability goals without acting as direct fertilizers or pesticides [9–11].

PBs can be naturally derived or synthetically formulated [12]. Among naturally derived PBs, volatile compounds (VCs) released by microorganisms, particularly fungi, have attracted increasing attention for their ability to promote plant growth and stress tolerance in a non-contact, low-input manner [13–16]. Fungal VCs are low-molecular-weight metabolites [17] that function as signaling molecules, triggering physiological and molecular responses that enhance plant growth, development, and stress tolerance [18–21]. In addition, fungal VCs can modulate plant-microbe interactions and influence ecosystem processes, suggesting their potential as sustainable alternatives or complements to conventional agrochemicals [22–25].

Numerous studies have reported that fungal VCs stimulate seed germination, root and shoot growth, and stress resilience across diverse plant species, and can also suppress plant pathogens [26–28]. For example, VCs emitted by fungi *Tolypocladium inflatum* GT22 significantly improved growth and mitigated copper toxicity and pathogenic infections in *Arabidopsis thaliana* [29]. In another study, VCs from fungal strains isolated from green manure residues showed dual functionality of promoting plant development while inhibiting pathogenic fungi [30]. Exposure to VCs from endophytic fungi, *Clonostachys sp*. CC1 and *sp*. CC2, promoted growth and biomass accumulation in rice and *Arabidopsis* [31]. Fungal VCs have been shown to stimulate plant growth through the activation of phytohormone signaling pathways, including auxin- and cytokinin-regulated processes [32,33]. They also induce systemic resistance by priming plants to produce defense-related molecules such as reactive oxygen species (ROS) and secondary metabolites [21,32]. In addition, fungal VCs can modulate stomatal conductance and enhance photosynthetic efficiency, contributing to improved physiological performance under stress [21,32]. Additional studies further support the potential of fungal VCs in enhancing agricultural productivity and underscoring their relevance in sustainable crop management strategies [34–36].

Despite these advances, the application of fungal VCs in agriculture remains limited. Key challenges include production cost, scalability, formulation, and delivery, as well as the lack of field-scale validation under realistic environmental conditions [32,37–39]. One potential solution is the use of agricultural waste streams as sources of bioactive volatiles. Waste shiitake fungi beds (WSFBs), a by-product of *Lentinula edodes* cultivation, represent a low-cost and renewable source of fungal VCs. Our preliminary findings reveal that non-contact exposure to WSFBs-derived VCs significantly boosts rice seedlings growth and biomass accumulation [40]. However, it remains unclear whether these early-stage effects persist after transplantation and translate into improved field performance, particularly under high temperature (HT) stress conditions.

We hypothesized that short-term exposure to WSFBs-derived VCs during the seedling stage would (i) enhance early vigor and improve key agronomic traits and yield components under field conditions across two contrasting growing seasons, and (ii) induce physiological and molecular responses associated with photosynthesis, stomatal regulation, and stress signaling. Accordingly, this study evaluated the effects of WSFBs-derived VCs on field performance of two *japonica* rice cultivars, Nipponbare and Koshihikari, while investigating underlying mechanisms through leaf gas-exchange measurements and expression analysis of growth and stress-related genes under acute HT stress assay. By linking multi-season field outcomes with mechanistic data, we extend our prior methodological work and assess the potential of WSFBs-derived VCs as practical, waste-based biostimulants for climate-resilient rice production.

2. Materials and Methods

2.1. Plant Materials, Fungi-Beds and Experimental Design

Two *O. sativa* L. japonica rice cultivars, Nipponbare and Koshihikari, were used in this study. WSFBs were obtained from Yairo Shiitake Business Cooperative (Niigata, Japan) after complete harvesting of *Lentinula edodes* Hokken 905 strain fruiting bodies (Hokken Corporation, Japan). WSFBs were stored at 10 °C and used within one-month post-harvest to maintain bioactive volatile compound (VC) emission.

2.2. Rice Seedling Cultivation and VCs Treatment

High-quality seeds were selected using the Tull salt-solution flotation method [41,42]. Rice seeds were immersed in a 25% (w/v) NaCl solution, and only those that sank were retained. Selected seeds were rinsed five times with tap water and three times with deionized water, treated with ipconazole (1:200 dilution; Kumiai Chemical Co. Ltd., Japan), and incubated in darkness at 15 °C for 11 days to allow imbibition and germination. Germinated seedlings were cultivated using a previously established non-contact VC exposure system [40]. Two treatments were applied: (i) +VCs, exposure to VCs emitted from 60 g fresh WSFBs substrate per container (~4.4 g FW L^{-1} air volume), and (ii) -VCs, untreated controls. Each treatment contained 40 seedlings grown in separate plastic containers (13.6 L, 38 × 22 × 24.8 cm; Daiso Industries Co. Ltd., Japan). Seedlings were grown in granular Kumiai synthetic culture soil No. 3 (1.50 g N, 2.70 g P, 1.50 g K per 3 kg; TAKARA Industry Co. Ltd., Japan). Soil pH was adjusted to that of calcium silicate following Kanga et al. (2025) [40]. Both treatments rice seedlings were cultivated for 31 days under controlled conditions (27 °C 13hrs. light and 23 °C 11hrs. dark; photosynthetic photon flux density (PPFD) of 123 ± 9 μmol m^{-2} s^{-1}; 60% relative humidity (RH)). The WSFB was replaced weekly.

2.3. Paddy Field Rice Seedlings Transplantation

Seedling vigor (shoot height, root length, dry weight) was assessed in a subset of seedlings ($n = 5$ per cultivar × treatment) before field transplantation. Remaining well grown seedlings were transplanted to paddy fields at Shindori Station, Field Center for Sustainable Agriculture, Niigata University (37°51′19″ N, 138°57′35″ E) from 15 May-30 September 2023 and 13 May-29 September 2024 (Figure S1). Transplanting followed a 30 × 30 cm spacing (one seedling per hill) in plots of 20 plants (~150 × 120 cm). Four treatments were established: Nipponbare -VCs/+VCs and Koshihikari -VCs/+VCs. Plots were separated by 100 cm buffers with a 180 cm southern walkway. Plots were used as treatment units, and individual plants served as experimental units for trait measurements. Seedlings were randomly assigned within plots to minimize positional bias. Standard rice cultivation practices were applied uniformly. Experimental timelines, workflow, and weather data are provided in Table S1, Figure S4, and Figure S2 respectively.

2.4. Analyses of Agronomic Traits of Rice Grown in Paddy Field

Agronomic traits were measured at physiological maturity after complete panicle emergence and grain filling. For each cultivar and season, five plants ($n = 5$) were randomly sampled from the interior of each plot to avoid border effects. We physically counted the number of tillers per plant, the number of panicles per plant, and the total number of spikelet and filled grains. Total grain weight per plant was measured after removing the husks of the rice seeds using electro motion rice husker TR-200 (Kett Electric Laboratory Co. Ltd. Japan). Yield related parameters were calculated as total grain weight per plant (g/plant). Seed fertility (%) was determined as (number of filled grains per plant / total spikelet number) × 100. Grain quality was assessed following Ishfaq et al. (2023) [43]. For each cultivar and treatment, three biological replicates (individual plants; $n = 3$) were analyzed. From each plant, 300 brown rice grains were sampled from the main culm and two randomly selected panicles. Chalkiness was evaluated under transmitted light using a FUJICOLOR LED light panel (Fujifilm Corporation, Japan; Model: MIVUKI) providing uniform, diffuse, and flicker-free illumination. Based on visual assessment, grains were categorized as (i) perfect (no chalkiness), (ii) weakly chalky (<60% chalky area), or (iii) severely chalky (≥60% chalky area) (Figure S3). Counts in each category were expressed as percentages of total grains. Two trained assessors independently performed the classifications, and discrepancies were resolved by consensus to minimize observer bias.

2.5. Photosynthesis and Leaf Gas Exchange Measurements

Leaf gas exchange measurements were conducted at the flowering stage (0 days after heading) using a portable photosynthesis system (LI-6400XT; LI-COR Environmental, Lincoln, NE, USA) equipped with a standard 2 × 3 cm leaf chamber (6 cm^2 gasket area), following Mathan et al. (2021) [44] with modifications. For each treatment, fully expanded flag leaves from field-grown plants were selected, and the middle portion of the leaf blade was positioned within the chamber to ensure full sealing and minimize air leakage. Measurements were performed under controlled chamber conditions with a CO_2 concentration of 400 μmol mol^{-1}, PPFD of 1200 μmol m^{-2} s^{-1}, leaf temperature maintained at 26 °C, and a flow rate of 400 μmol s^{-1}. Relative humidity was maintained between 45% and 50%. Gas exchange measurements were conducted on clear, sunny days between 14:00 and 16:00 h. Measurements in this study were performed during early afternoon to capture stable high-light conditions during the warmer 2023 growing season. Given the narrow width of rice flag leaves (<2 cm), actual leaf area enclosed within the chamber was corrected using a width-based geometric approach [45]. Leaf width (W, cm) at the chamber center was measured using digital calipers, and effective leaf area was calculated as: $\text{Area } (cm^2) = 6 \times [1 - (1 - W/3)^2]$, where W is leaf width (cm) measured with calipers at the chamber center. This correction accounted for partial chamber filling and resulted in a mean adjustment factor of approximately 2.5-3× relative to the LI-6400XT default estimated area (1-1.4 cm^2). All gas exchange parameters were normalized to this corrected leaf area. The parameters recorded included: net photosynthetic rate (A_n; μmol CO_2 m^{-2} s^{-1}), stomatal conductance (g_s; mol m^{-2} s^{-1}), transpiration rate (E; mmol H_2O m^{-2} s^{-1}) , intercellular CO_2 concentration (C_i; μmol mol^{-1}) and intrinsic water use efficiency (WUE) was calculated as the ratio of A_n to g_s. For each leaf, multiple readings were recorded, and values were averaged after A_n, g_s, and C_i reached a stable plateau. Only physiologically consistent readings (i.e., positive and stable values for A_n, g_s, C_i, and E) were included in the final analysis. Measurements from multiple leaves were treated as biological replicates and used for subsequent statistical analysis.

2.6. High Temperature Stress Test at the Rice Seedling Stage

To characterize early physiological and transcriptional responses to WSFBs-derived VCs at the seedling stage, a controlled acute HT stress experiment was conducted. This assay was designed to provide mechanistic insight into seedling-stage responses to WSFBs-derived VCs. Rice seeds (*O. sativa* L. cv. Nipponbare) were surface-sterilized with 2% sodium hypochlorite, germinated for four days at 28 °C (13 hrs. light/11 hrs. dark), and transplanted into sterile soil-filled Magenta boxes. Seedlings were grown for 14 days under the non-contact VCs exposure system under conditions described in 2.2 above (27 °C 13 hrs. light and 23 °C 11 hrs. dark; 123 ± 9 μmol m^{-2} s^{-1} PPFD; 60% RH). Based on a previously optimized non-contact exposure system [40], +VCs seedlings were cultivated in sealed 3 L containers with 60 g fresh WSFB substrate, while -VCs seedlings were maintained in identical containers without WSFB. Following the exposure period, seedlings were subjected to a 24 h acute HT treatment consisting of 45 °C for 13 hrs. light, followed by 38 °C for 11 hrs. dark, based on established rice heat-tolerance protocols [46–48]. Three biological replicates (n = 3) were collected per treatment at each sampling time point.

After HT treatment, seedling growth and physiological traits were assessed. Growth parameters (dry weight, shoot height, and root length) were measured following Kanga et al. (2025) [40]. Physiological measurements included SPAD values (SPAD-502 Plus; Konica Minolta, Japan), malondialdehyde (MDA) content, and chlorophyll content [49,50]. For MDA quantification, 50 mg fresh leaf tissue was homogenized in 2 mL of 10% (w/v) trichloroacetic acid (TCA) and centrifuged at 12,500 rpm for 20 min at room temperature. One milliliter (mL) of supernatant was mixed with 1 mL of TCA-thiobarbituric acid (TBA) reagent [1:1 (v/v); 10% TCA + 0.5% TBA], incubated at 90 °C for 30 min, and cooled on ice. Absorbance was measured at 532 nm and 600 nm using a UV-Vis spectrophotometer (Hitachi U-2900; Hitachi High-Technologies, Japan). MDA content (nmol g^{-1} FW) was calculated as: $\text{MDA} = [(A_{532} - A_{600}) \times V] / (\varepsilon \times l \times W)$, where $\varepsilon = 155$ mM^{-1} cm^{-1}, V is the reaction volume (mL), l is the path length (1 cm), and W is tissue fresh weight (g). Chlorophyll content was determined using an acetone extraction method [51]. Fresh leaf tissue (50 mg) was homogenized and extracted in 2 mL of 80% (v/v) acetone under low-light conditions to prevent pigment degradation. Samples were centrifuged, and the supernatant was collected for spectrophotometric analysis. Absorbance was measured at 664 nm and 647 nm using a UV-Vis spectrophotometer (Hitachi U-2900, Japan). Chlorophyll a, chlorophyll b, and total chlorophyll concentrations were calculated according to Lichtenthaler and Wellburn [50] using the following equations:

- Chlorophyll a (Chl a) = $12.25 \times A_{664} - 2.79 \times A_{647}$
- Chlorophyll b (Chl b) = $21.50 \times A_{647} - 5.10 \times A_{664}$
- Total chlorophyll (Chl a + b) = $7.15 \times A_{664} + 18.71 \times A_{647}$

Chlorophyll content was expressed as mg g^{-1} fresh weight (FW) using:

$$\text{Chl (mg g}^{-1}\text{ FW)} = (C \times V) / W$$

where C is chlorophyll concentration (mg L^{-1}), V is extract volume (2 mL), and W is sample fresh weight (g).

For RNA extraction and qPCR analysis, plant samples collected at 0, 6, 12, and 24 hrs. after HT treatment were immediately frozen in liquid nitrogen and stored at –80 °C. Total RNA was extracted using the RNeasy Plant Mini Kit (QIAGEN) according to the manufacturer's protocol. First-strand cDNA was synthesized using ReverTra Ace qPCR RT Master Mix with gDNA remover (TOYOBO, Japan). Quantitative PCR (qPCR) was performed using a StepOnePlus Real-Time PCR system (Thermo Fisher Scientific) with PowerTrack SYBR Green Master Mix. Relative gene expression was calculated using the $2^{-\Delta\Delta Ct}$ method [52], with UBQ5 as the internal reference gene (Table S6). Primer efficiencies were validated and confirmed to be within acceptable ranges for the $2^{-\Delta\Delta Ct}$ method. All reactions were performed in technical triplicates, and mean Ct values were used for analysis. A schematic overview of the experimental workflow is provided in Figure S5.

2.7. Statistical Analysis

Data were organized in Microsoft Excel 365. For pairwise comparisons between treatments (+VCs vs. -VCs) within each cultivar and year, two-tailed Student's *t*-tests were performed, with $p < 0.05$ considered statistically significant. Results are presented as mean ± standard deviation (SD). Multivariate analyses were conducted in R (version 3.6.1; R Core Team, https://www.r-project.org/). Principal component analysis (PCA) was used to assess relationships among physiological, agronomic, and yield variables. Hierarchical clustering analysis (HCA) was performed using Ward's method and Euclidean distance. Given the modest sample sizes (n = 5 for field data; n = 3 for controlled experiments), interpretation emphasized effect sizes, biological relevance, and reproducibility across years.

3. Results

3.1. Field Performance of Rice Following Exposure to WSFBs-Derived VCs Exposure

Field experiments were conducted in Niigata, Japan, to evaluate whether seedling-stage exposure to WSFBs-derived VCs influences rice performance under field conditions. The 2023 season experienced anomalously high summer temperatures (maximum 39.1 °C), whereas 2024 was comparatively moderate (Tables S2, S3). These contrasting conditions enabled assessment of treatment responses under both severe and mild thermal environments.

3.1.1. Seedling Vigor After Exposure to WSFBs-Derived VCs Prior to Paddy Transplantation

After 31 days of exposure, +VCs seedlings exhibited greater biomass accumulation than -VCs controls in both cultivars (Figure S7). In Nipponbare, dry weight increased by 57.1% (157.0 ± 40.9 mg to 246.6 ± 74.0 mg; $p < 0.05$), accompanied by a 35.6% increase in root length (8.26 ± 1.38 cm to 11.20 ± 1.54 cm; $p < 0.05$). Shoot height did not differ significantly. In Koshihikari, dry weight increased by 75.5% (158.2 ± 24.4 mg to 277.6 ± 48.1 mg; $p < 0.01$), while shoot height and root length remained unchanged. These results indicate that biomass responses were more consistently expressed in dry weight than in shoot or root elongation.

3.1.2. Heading Dates

Seedling-stage exposure to WSFBs-derived VCs influenced heading date primarily during the 2023 growing season (Table S2). In 2023, +VCs plants headed earlier than -VCs plants in both cultivars (Nipponbare: 16th vs. 22nd August; Koshihikari: 28th July vs. 2nd August). This shift in phenology corresponded with differences in environmental conditions during the heading window (Table S3A). In Nipponbare, +VCs plants experienced a lower mean maximum temperature (T_{max}) during heading (26.4 °C) compared with -VCs plants (27.3 °C). Similarly, in Koshihikari, +VCs plants headed under a lower T_{max} (25.3 °C) compared with -VCs plants (26.4 °C). Seasonal temperature trends during 2023, characterized by a progressive rise toward peak summer conditions, are shown in Figure S2A. In contrast, during the 2024 growing season, heading differences between treatments were minimal (≤1 day) in both cultivars (Table S2). Environmental conditions during the heading period were also comparable between treatments, with nearly identical T_{max} values observed in both Nipponbare (26.0-26.1 °C) and Koshihikari (25.8-25.9 °C) (Table S3B; Figure S1B). These results indicate that WSFBs-derived VCs exposure was associated with earlier heading under the 2023 conditions, whereas no consistent differences were observed under the milder 2024 season.

3.1.3. Tiller and Panicle Number

Tiller number per plant was higher in +VCs plants across cultivars and seasons (Figure 1A, B). In Nipponbare, +VCs plants produced 39.0 ± 6.6 tillers in 2023 compared with 33.0 ± 5.5 in -VCs plants (+18.9%; $p = 0.145$) and 37.0 ± 6.9 vs. 27.0 ± 4.6 in 2024 (+39.9%; $p = 0.021$). In Koshihikari, increases were 27.2% in 2023 (43.0 ± 4.9 vs. 34.0 ± 5.5; $p = 0.023$) and 42.9% in 2024 (28.0 ± 4.9 vs. 20.0 ± 2.9; $p = 0.011$). Panicle number followed a similar pattern (Figure 1C,D). In Nipponbare, +VCs plants produced 38.0 ± 5.6 panicles in 2023 vs. 31.0 ± 5.5 in –VCs plants (+24.8%; $p = 0.062$) and 36.0 ± 6.4 vs. 26.0 ± 4.3 in 2024 (+37.9%; $p = 0.020$). In Koshihikari, increases were 25.0% in 2023 (41.0 ± 6.0 vs. 33.0 ± 5.6; $p = 0.056$) and 52.8% in 2024 (27.0 ± 5.7 vs. 18.0 ± 3.5; $p = 0.014$).

3.1.4. Seed Fertility and Total Grain Weight

Seed fertility was numerically higher in +VCs plants across cultivars and seasons, although differences were not statistically significant (Figure 1E,F). In Nipponbare, fertility increased by 2.9% in 2023 (86.6 ± 3.1% vs. 84.2 ± 2.8%; $p = 0.232$) and 0.7% in 2024 (93.5 ± 4.9% vs. 92.8 ± 1.4%; $p = 0.782$). In Koshihikari, increases were 7.9% in 2023 (92.5 ± 3.8% vs. 85.7 ± 8.5%; $p = 0.142$) and 1.4% in 2024 (95.2 ± 1.5% vs. 93.9 ± 1.2%; $p = 0.172$). Total grain weight per plant was higher in +VCs plants in all cases (Figure 1I,J). In Nipponbare, increases were 26.0% in 2023 (83.3 ± 13.2 g vs. 66.1 ± 10.4 g; $p = 0.051$) and 20.7% in 2024 (68.6 ± 24.3 g vs. 56.8 ± 8.6 g; $p = 0.339$). In Koshihikari, increases were 68.6% in 2023 (88.9 ± 17.6 g vs. 52.7 ± 18.6 g; $p = 0.013$) and 84.8% in 2024 (73.8 ± 17.8 g vs. 39.9 ± 6.7 g; $p = 0.004$)

3.1.5. 1000-Grain Weight

The 1000-grain weight (OTGW) was significantly higher in +VCs plants across cultivars and seasons (Figure 1G,H). In Nipponbare, OTGW increased by 5.5% in 2023 (21.0 ± 0.5 g to 22.0 ± 0.5 g; $p = 0.0066$) and 6.6% in 2024 (22.0 ± 0.2 g to 23.0 ± 0.2 g; $p < 0.001$). In Koshihikari, increases were 4.4% in 2023 (20.0 ± 0.3 g to 21.0 ± 0.5 g; $p = 0.010$) and 4.9% in 2024 (21.0 ± 0.3 g to 22.0 ± 0.3 g; $p < 0.001$). These increases were statistically significant in all comparisons.

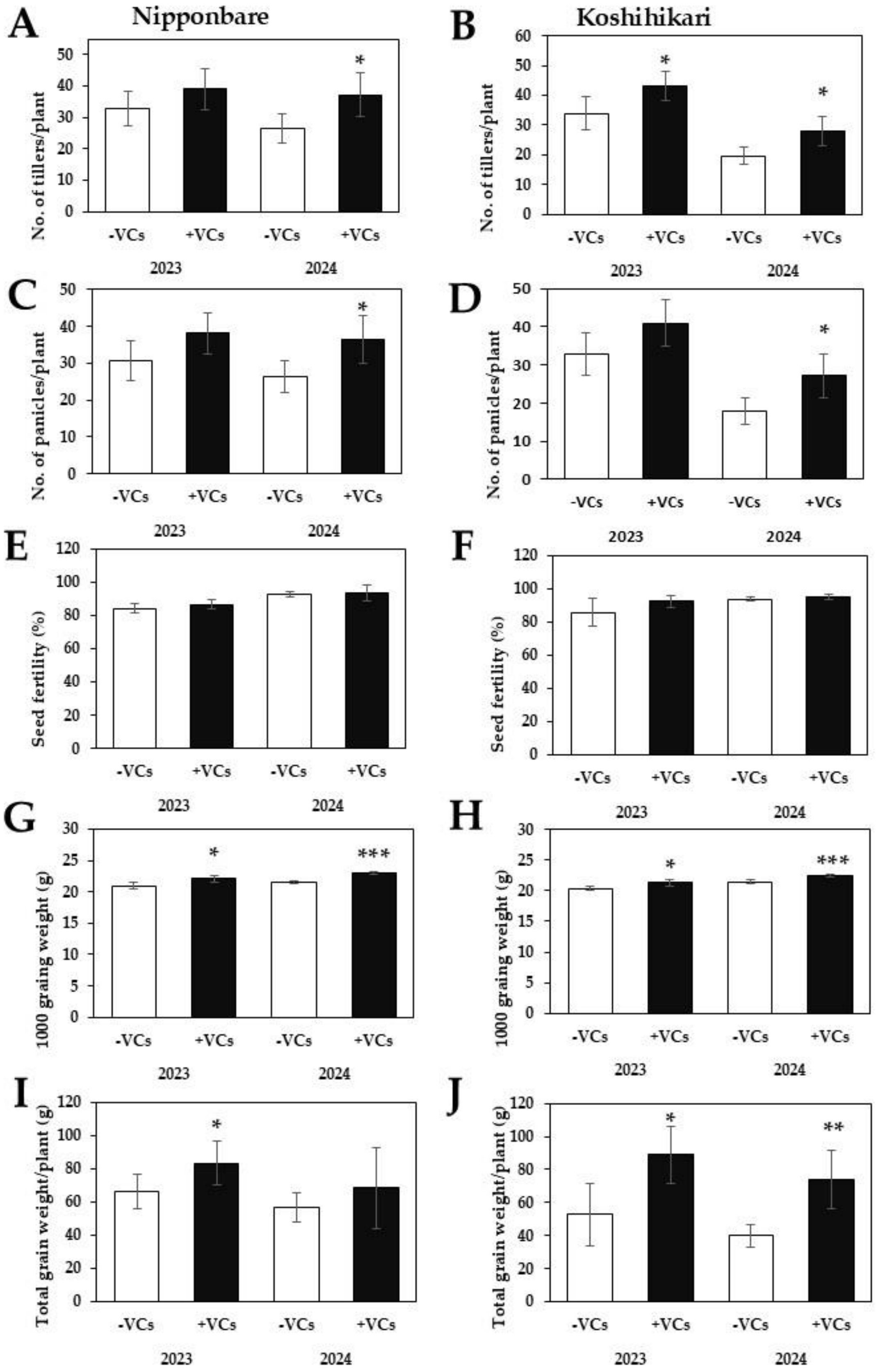

Figure 1. Yield-related agronomic traits in rice cultivars Nipponbare (left) and Koshihikari (right) following exposure to WSFBs-derived VCs (+VCs) compared with untreated controls (-VCs) during the 2023 and 2024 growing seasons. (A-B) Tillers per plant; (C-D) panicles per plant; (E-F) seed fertility; (G-H) 1000-grain weight; (I-J) total grain weight per plant. Bars represent averages ± SD (n = 5). White bars indicate -VCs and black bars

indicate +VCs treatments. Asterisks denote significant differences between treatments (*p < 0.05; **p < 0.01; ***p < 0.001; Student's t-test).

3.1.6. Grain Quality

Grain quality parameters differed between treatments across both cultivars and growing seasons (Figure 2). In Nipponbare, the proportion of perfect grains in +VCs plants was 7.0% higher than in -VCs plants in 2023 (65.0% vs. 58.0%), accompanied by a 2.0% reduction in moderately chalky grains (33.0% vs. 35.0%) and a 5.0% reduction in severely chalky grains (2.0% vs. 7.0%) (Figure 2A). A similar pattern was observed in 2024, where perfect grains were higher by 7.0% (68.0% vs. 61.0%), moderately chalky grains decreased by 3.0% (31.0% vs. 34.0%), and severely chalky grains declined by 4.0% (1.0% vs. 5.0%). In Koshihikari, the proportion of perfect grains in +VCs plants was 4.0% higher than in -VCs plants in 2023 (64.0% vs. 60.0%), while moderately chalky grains remained similar (35.0% vs. 34.0%). Notably, severely chalky grains were reduced by 5.0% (1.0% vs. 6.0%) (Figure 2B). In 2024, perfect grains increased by 4.0% (67.0% vs. 63.0%), moderately chalky grains decreased slightly by 1.0% (32.0% vs. 33.0%), and severely chalky grains declined by **3.0%** (1.0% vs. 4.0%). Across both cultivars and growing seasons, +VCs plants consistently exhibited higher proportions of perfect grains and lower proportions of severely chalky grains compared with -VCs plants.

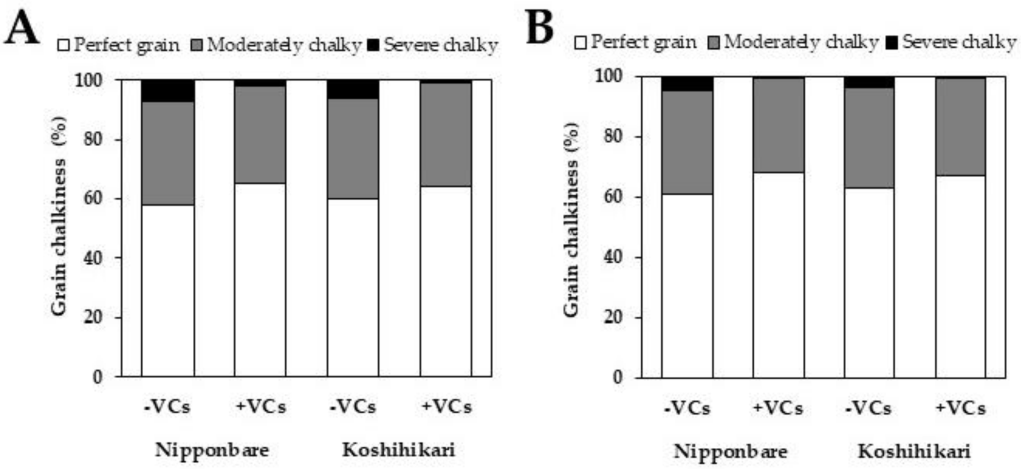

Figure 2. Grain quality composition in rice cultivars Nipponbare and Koshihikari exposed to WSFBs-derived VCs (+VCs) and untreated controls (-VCs) during the 2023 (A) and 2024 (B) growing seasons. Bars show the proportions of perfect grains (white), moderately chalky grains (gray), and severely chalky grains (black). Values represent average proportions from three independent biological replicates.

3.2. Physiological Mechanisms of How WSFBs-Derived VCs-Mediated HT Stress Tolerance

3.2.1. WSFBs-Derived VCs Promoted Photosynthetic Activities Under HT Stress Conditions

To understand the physiological basis for the improved growth, yield, and grain quality observed in +VCs plants under HT field conditions in 2023, we analyzed photosynthetic and gas exchange parameters in transplanted rice plants (Figure 3). Net photosynthetic rate (A_n) was consistently higher in +VCs plants than in -VCs plants in both cultivars. In Nipponbare, A_n was 27.9% higher in +VCs plants than in -VCs plants (21.4 ± 1.0 vs. 27.4 ± 1.0 μmol CO_2 m^{-2} s^{-1}; $p < 0.001$), while in Koshihikari it increased by 58.4% (15.1 ± 0.8 vs. 24.0 ± 1.2 μmol CO_2 m^{-2} s^{-1}; $p < 0.001$) (Figure 3A). Stomatal conductance (g_s) showed a similar pattern. Nipponbare exhibited a 64.2% increase in g_s in +Vs plants over the -VCs plants (0.7 ± 0.2 vs. 1.2 ± 0.3 mol m^{-2} s^{-1}; $p < 0.001$), while Koshihikari showed a 36.1% increase (0.9 ± 0.2 vs. 1.3 ± 0.2 mol m^{-2} s^{-1}; $p < 0.01$) (Figure 3B). Intercellular CO_2 concentration (C_i) was also significantly elevated in +VCs plants. Nipponbare showed an 81.7% increase in +VCs plants over the -VCs plants (128.0 ± 11.0 vs. 233.0 ± 7.0 μmol mol^{-1}; $p < 0.001$), and Koshihikari showed an 83.5% increase (122 .0± 4.0 vs. 225 .0± 9.0 μmol mol^{-1}; $p < 0.001$) (Figure 3C). Transpiration rate (E) followed the same trend, with +VCs plants exhibiting a 48.5% increase in Nipponbare (10.6 ± 1.8 vs. 15.7 ± 2.1 mmol H_2O m^{-2} s^{-1}; $p < 0.001$) and a 73.7% increase in Koshihikari (7.5 ± 0.7 vs. 13.0± 1.6 mmol H_2O m^{-2} s^{-1}; $p < 0.001$) (Figure 3D). In contrast, intrinsic water-use efficiency (WUE) showed a modest, non-significant decline in +VCs plants. WUE decreased by 15.2% in Nipponbare (2.10 ± 0.46 to 1.78 ± 0.28; $p = 0.056$) and by 8.7% in Koshihikari (2.1± 0.3 to 1.97 ± 0.2; $p = 0.111$) (Figure 3E). Overall, WSFB-derived VCs enhanced A_n, g_s, C_i, and E in both cultivars, while WUE exhibited a slight but non-significant reduction.

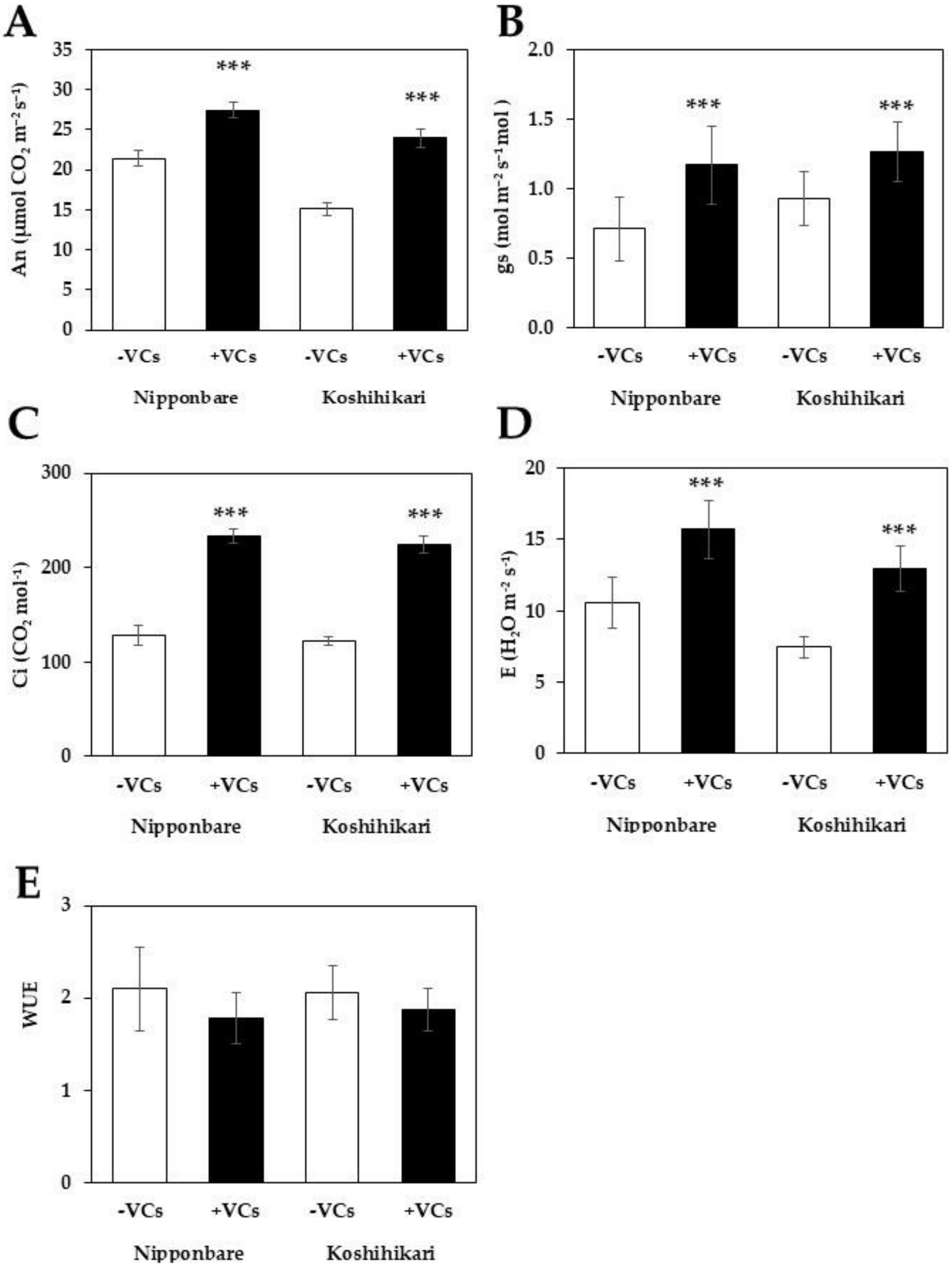

Figure 3. Gas exchange parameters in rice cultivars Nipponbare and Koshihikari treated with WSFBs-derived VCs (+VCs) and untreated controls (–VCs). White bars represent -VCs and black bars represent +VCs. Each bar represents the average ± SD of three independent biological replicates. Asterisks indicate significant differences between -VCs and +VCs calculated by Student's t-test (*$p < 0.05$; **$p < 0.01$; ***$p < 0.001$).

3.3. Controlled-Environment Analyses Reveal Physiological and Transcriptional Responses Associated with VCs Exposure Under Acute HT Stress

While field experiments showed that WSFBs-derived VCs enhanced rice performance under natural HT conditions in 2023, controlled-environment assays were conducted to examine associated physiological and molecular responses under defined stress conditions.

3.3.1. Growth and Physiological Responses Under Acute HT Stress

Prior exposure of rice seedlings (*O. sativa* L. cv. Nipponbare) to WSFBs-derived VCs (+VCs) for 14 days followed by a 24 hrs acute HT treatment (45 °C 13 hrs. light, followed by 38 °C 11 hrs. dark) resulted in improved growth performance compared with untreated controls (-VCs) (Table S4; Figure S6). Visually, +VCs seedlings maintained greener leaves and greater biomass following HT exposure. Quantitative analysis confirmed that dry weight was significantly higher in +VCs seedlings (3.7-fold increase relative to -VCs; $p < 0.001$, Figure S6 B), while shoot height showed a modest but significant increase (1.2-fold; $p < 0.001$, Figure S6 C). Root length did not differ significantly between treatments. Physiological measurements further indicated improved stress tolerance in +VCs seedlings. SPAD values were significantly higher in +VCs plants (33.4 ± 3.8) compared with -VCs plants (17.6 ± 5.0; $p < 0.01$), indicating greater chlorophyll retention under HT stress (Figure S6 E). In addition, MDA content was significantly lower in +VCs seedlings ($p < 0.01$, Figure S6 I), suggesting reduced lipid peroxidation and membrane damage. Consistently, chlorophyll a, chlorophyll b, and total chlorophyll contents were significantly higher in +VCs seedlings, increasing by 73.2%, 81.8%, and 76.8%, respectively ($p < 0.001$) (Figure S6 F, G, H), indicating reduced chlorophyll degradation under HT stress. Together, these results indicate that WSFBs-derived VCs exposure is associated with improved physiological stability of rice seedlings under acute HT stress, characterized by enhanced biomass accumulation, reduced oxidative damage, and improved chlorophyll retention.

3.3.2. WSFBs-Derived VCs Enhance Cytokinin Signaling Under HT Stress

To examine molecular responses underlying the observed physiological differences, we quantified the expression of four cytokinin-responsive genes (*OsRR4*, *OsRR6*, *OsRR9*, and *OsRR10*) under HT stress, selected as markers of cytokinin signaling under abiotic stress [53,54]. Overall, transcript levels of these OsRR genes were higher in +VCs than in -VCs plants at most time points, with the clearest differences during the initial 6-12 hrs. of HT exposure.

OsRR4 expression declined over time in both treatments but remained significantly higher in +VCs plants at 6 hrs. (1.2 ± 0.1 vs. 0.7 ± 0.1, $p = 0.002$; ~1.6-fold) and 12 hrs. (1.00 ± 0.07 vs. 0.3 ± 0.0, $p < 0.001$; ~3.0-fold), whereas differences at 0 hrs. and 24 hrs. were not significant (Figure 4A). *OsRR6* showed the strongest and most sustained response, with +VCs plants displaying markedly higher expression at 0 hrs. (4.1 ± 0.2 vs. 1.1 ± 0.6, $p = 0.001$), 6 h (4.8 ± 0.4 vs. 2.0 ± 0.1, $p < 0.001$), and 12 hrs. (3.7 ± 0.5 vs. 2.1 ± 0.7, $p = 0.026$), while the difference at 24 hrs. was not significant. (Figure 4B). *OsRR9* and *OsRR10* showed similar temporal trends, with progressive downregulation in -VCs plants and higher early expression in +VCs plants. For *OsRR9*, +VCs plants had significantly higher transcript levels at 6 h (3.4 ± 0.9 vs. 0.5 ± 0.1, $p = 0.028$) and 24 hrs. (0.8 ± 0.1 vs. 0.4 ± 0.0, $p < 0.001$), but not at 0 hrs. or 12 hrs. (Figure 4C). For *OsRR10*, expression in +VCs plants was significantly elevated at 0 hrs. (2.2 ± 0.3 vs. 1.0 ± 0.2, $p = 0.0048$), 6 hrs. (2.1 ± 0.3 vs. 0.5 ± 0.1, $p = 0.0014$), and 24 hrs (0.8 ± 0.1 vs. 0.4 ± 0.0, $p = 0.0004$), with no significant difference at 12 hrs (Figure 4D).

Together, these data indicate that WSFBs-derived VCs promote an enhanced, early activation of cytokinin-responsive gene expression under HT stress, particularly within the first 6-12 hrs after stress onset.

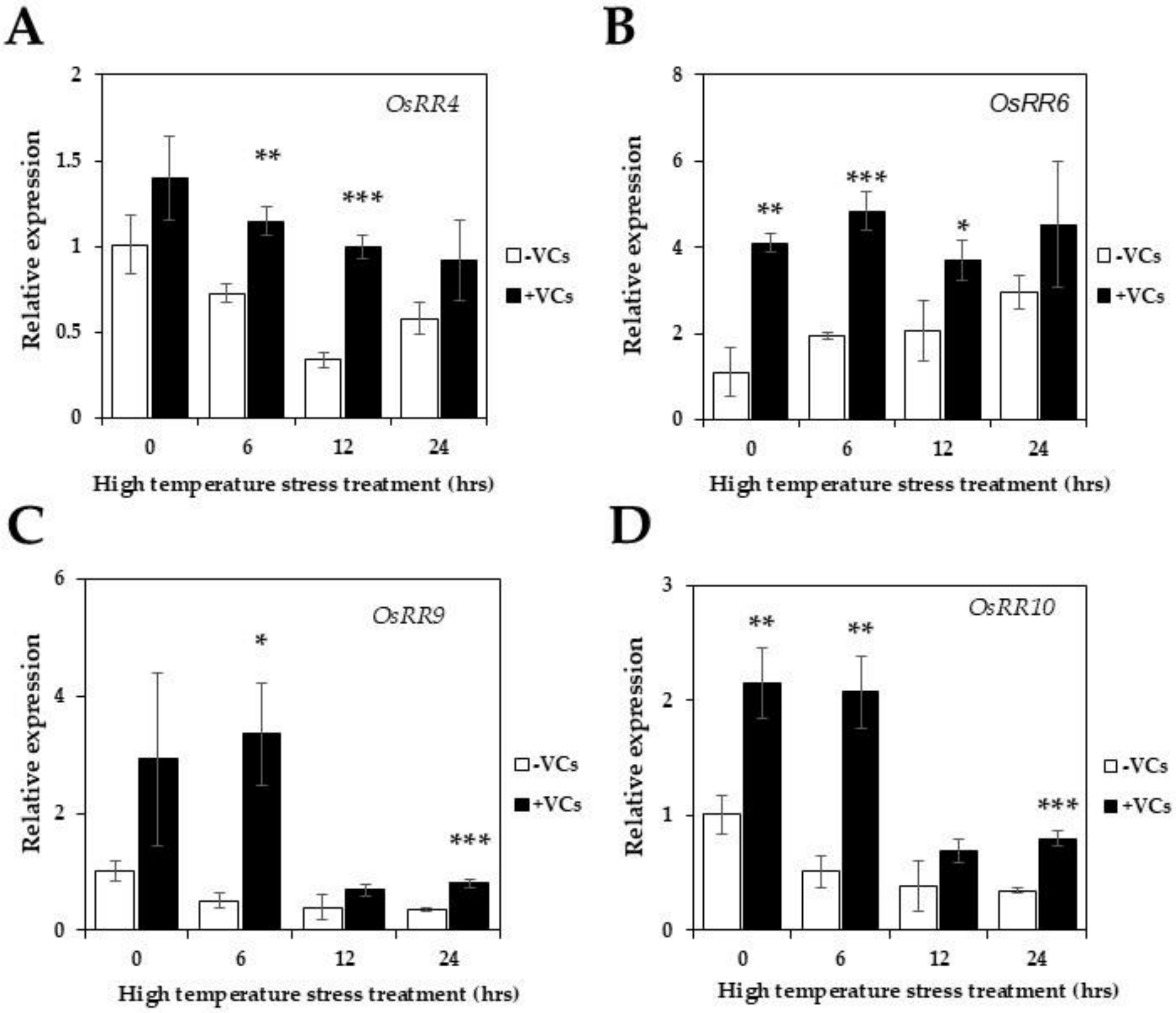

Figure 4. Relative expression of cytokinin signaling pathway genes in rice seedlings exposed to VCs derived from WSFBs under HT stress. Gene expression levels of *OsRR4* (A), *OsRR6* (B), *OsRR9* (C), and *OsRR10* (D) were analyzed in Nipponbare rice seedlings treated with WSFBs-derived VCs (+VCs) and untreated seedlings (-VCs) at 0, 6, 12, and 24 hrs after HT stress exposure. White bars represent -VCs and black bars represent +VCs. Data are presented as average ± SD (n=3). Asterisks indicate statistically significant differences between -VCs and +VCs determined by Student's t-test (* $p < 0.05$; ** $p < 0.01$; *** $p < 0.001$).

3.3.3. WSFB-Derived VCs Modulate Stress-Responsive and Redox-Related Gene Expression Under HT Stress

To further clarify the molecular basis of WSFBs-derived VCs mediated stress responses, we examined the expression of antioxidant and stress-related genes, including *OsGSTU6*, *OsGRXS17*, *OsDHAR1*, *OsSLAC1*, and *OsSNAC1* (Figure 4). These genes were selected based on their well-established roles in abiotic stress adaptation. *OsGSTU6* and *OsGRXS17* participate in oxidative stress defense by modulating ROS detoxification and redox buffering capacity [55,56]. *OsSLAC1* encodes a slow anion channel critical for ion transport and stomatal conductance regulation under stress conditions [57]. *OsDHAR1* contributes to redox homeostasis through its function in the ascorbate-glutathione cycle, enhancing ascorbate recycling and ROS scavenging [58]. *OsSNAC1*, a well-characterized NAC transcription factor, functions as a key regulator of drought-responsive gene networks and stomatal behavior [59,60]. Overall, all genes showed higher transcript levels in +VCs than in -VCs plants, particularly during the early phase of HT stress (0-12 h), consistent with a primed stress-response state.

OsGSTU6 was markedly upregulated in +VCs plants at 0 hrs. (2.6 ± 0.1 vs. 1.0 ± 0.1, $p < 0.001$), 12 hrs. (3.7 ± 0.9 vs. 1.2 ± 0.4, $p = 0.0089$), and 24 hrs. (2.6 ± 0.4 vs. 1.5 ± 0.5, $p = 0.0357$), whereas the difference at 6 hrs. was not significant despite higher mean expression in +VCs plants (Figure 5A). Similarly, *OsGRXS17* transcript levels were significantly higher in +VCs plants at 0 h (2.9 ± 0.3 vs. 1.0 ± 0.2, $p = 0.001$), 6 hrs. (2.5 ± 0.4 vs. 1.2 ± 0.1, $p = 0.0044$), and 12 hrs. (1.4 ± 0.1 vs. 0.3 ± 0.1, $p < 0.001$), but not at 24 hrs., pointing to early activation of redox homeostasis (Figure 5B). *OsSLAC1*, linked to stomatal regulation, showed significantly higher expression in +VCs plants at 6 hrs. (1.2 ± 0.2 vs. 0.7 ± 0.0, $p = 0.0179$) and 12 hrs. (0.8 ± 0.2 vs. 0.1 ± 0.0, $p = 0.0043$), while 0 hrs. and 24 hrs. differences were not significant (Figure 5C). *OsDHAR1* displayed the strongest induction among all genes analyzed. At 0 hrs., +VCs plants showed markedly higher expression than -VCs plants (7.3 ± 0.2 vs. 1.1 ± 0.5, $p < 0.001$), indicating robust basal activation of antioxidant capacity, and this difference remained significant at 24 hrs. (5.1 ± 0.8 vs. 2.0 ± 0.6, $p = 0.0052$) (Figure 5D). *OsSNAC1* expression was significantly higher in +VCs plants at 6 h (2.1 ± 0.3 vs. 0.5 ± 0.1, $p = 0.0006$), 12 hrs. (1.7 ± 0.2 vs. 0.9 ± 0.1, $p = 0.0033$), and 24 hrs. (4.1 ± 0.7 vs. 1.5 ± 0.3, $p = 0.004$), with the strongest induction at 24 hrs., indicating sustained activation of stress-responsive transcription (Figure 5E). Although +VCs plants also tended to have higher *OsDHAR1* expression at 6 hrs. and 12 hrs., these differences were not statistically significant. Together, these findings show that WSFBs-derived VCs enhance the activation of stress-responsive, antioxidant, and redox-regulating pathways under HT stress, particularly during early stress phases, supporting a priming effect that likely contributes to improved stress tolerance.

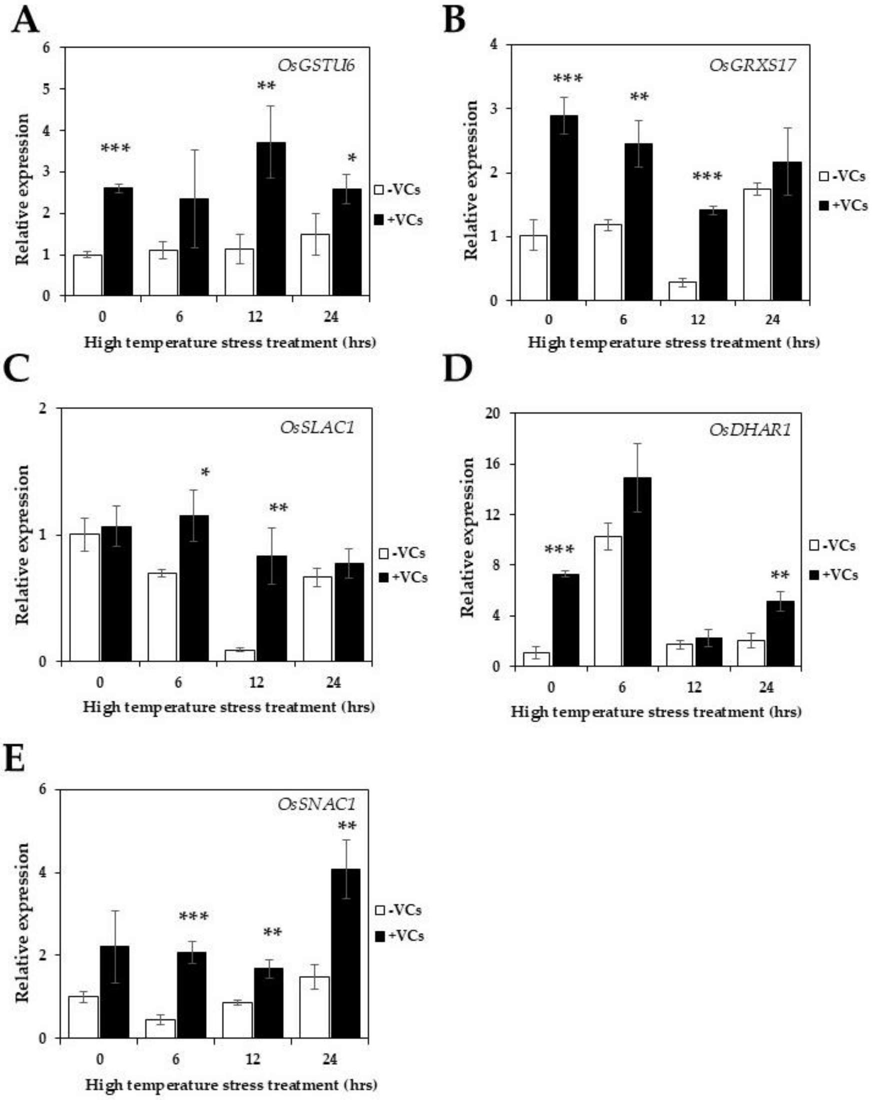

Figure 5. Relative expression of antioxidant- and stress-responsive genes in rice seedlings treated with VCs derived from WSFBs under HT stress. Gene expression levels of *OsGSTU6* (A), *OsGRXS17* (B), *OsSLAC1* (C), *OsDHAR1* (D), and *OsSNAC1* (E) were analyzed in Nipponbare rice seedlings treated with WSFBs-derived VCs (+VCs) and untreated seedlings (-VCs) at 0, 6, 12, and 24 hrs after HT stress exposure. White bars represent -VCs and black bars represent +VCs. Data are presented as average ± SD (n=3). Asterisks indicate statistically significant differences between -VCs and +VCs determined by Student's t-test (* $p < 0.05$; ** $p < 0.01$; *** $p < 0.001$).

3.4. Principal Component Analysis Reveals Treatment-Driven Separation of +VCs Plants

Principal component analysis (PCA) was performed to evaluate the combined effects of WSFBs-derived VCs on growth and physiological traits in Nipponbare and Koshihikari under HT conditions in 2023 (Figure 6A). The first two principal components explained most of the variation in the dataset, with PC1 accounting for 66.8% and PC2 for 16.3% of the total variance (83.1% cumulative). A clear separation between +VCs and -VCs plants was observed along PC1 (Figure 6A), indicating that WSFBs-VCs treatment was the primary source of variation. Samples from both Nipponbare and Koshihikari under +VCs clustered on the positive side of PC1, whereas -VCs samples were positioned on the negative side. This consistent separation across cultivars suggests that the effect of WSFBs-VCs treatment was robust and largely independent of genetic background.

The contribution of individual traits to this separation is shown in the PCA loading plot (Figure 6B). Photosynthesis (A_n), transpiration rate (E), intercellular CO_2 concentration (C_i), and total grain weight per plant were strongly aligned with the positive direction of PC1, indicating that these traits were the main drivers of the +VCs cluster. In contrast, tiller number, panicle number, and stomatal conductance contributed more to variation along PC2, reflecting secondary differences among treatments and cultivars.

Hierarchical clustering analysis (HCA) further supported these patterns (Figure 6C). The heatmap grouped samples primarily according to treatment, with +VCs plants from both cultivars clustering together and showing higher average values for most physiological and yield-related traits. In contrast, VCs plants formed a separate cluster characterized by comparatively lower trait values.

Overall, these multivariate analyses demonstrate that exposure to WSFB-derived volatile compounds induced a coordinated enhancement of physiological performance and yield-related traits. Importantly, this response was consistent across both Nipponbare and Koshihikari, highlighting the broad and reproducible effect of VCs under high-temperature field conditions.

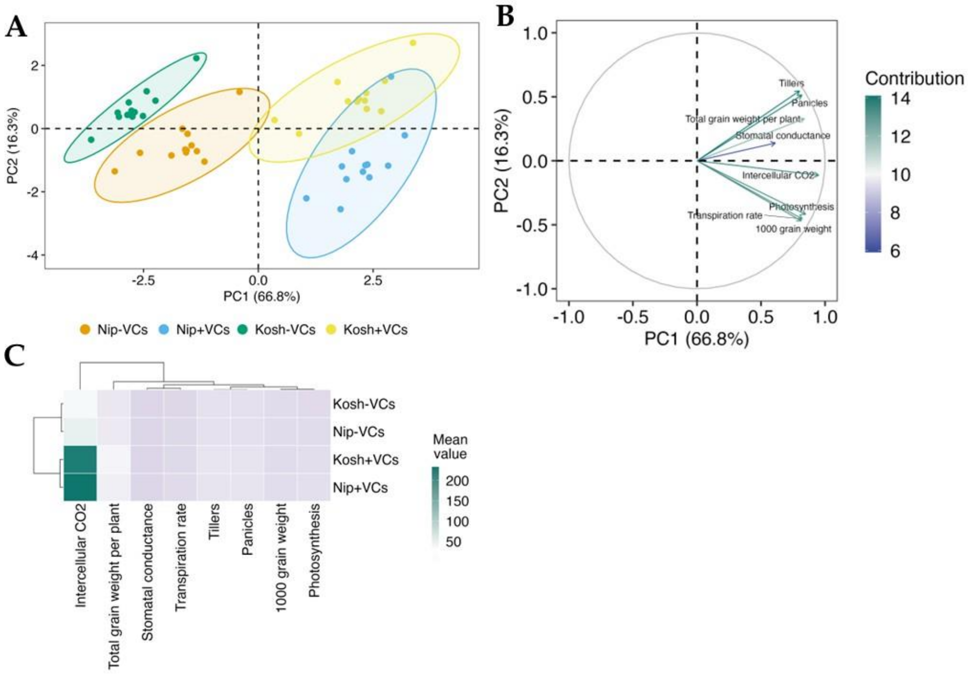

Figure 6. Multivariate analysis of physiological and agronomic traits in Nipponbare and Koshihikari under WSFB-derived VCs treatment for 2023 growing season. (A) PCA score plot showing separation of +VCs and -VCs samples along PC1 (66.8%), with PC2 (16.3%) reflecting secondary variation. (B) PCA loading plot indicating VCs contributions to traits, with photosynthesis (A_n), transpiration rate (E), intercellular CO_2 concentration (C_i), and grain weight associated with the positive direction of PC1. (C) Hierarchical clustering heatmap showing treatment-dependent patterns, where +VCs samples cluster together and exhibit higher trait values than -VCs controls.

4. Discussion

Field-Scale Evaluations: Growth, Yield, and Grain Quality Under Natural HT Stress

Our previous work established that rice seedlings can perceive VCs emitted from WSFBs and respond with enhanced early growth under controlled conditions [40]. The present study extends these findings to field environments and demonstrates that a short seedling-stage exposure to WSFBs-derived VCs can influence subsequent growth, development, and yield formation in two *japonica* cultivars. Across two growing seasons with contrasting thermal regimes, +VCs plants consistently exhibited greater early vigor, increased tiller and panicle production, and higher grain yield compared with -VCs plants.

The early enhancement of seedling biomass and root growth likely provided a physiological advantage that supported stronger establishment and resilience after transplanting. This early-stage vigor offers a plausible mechanistic link to the increased tillering, panicle number, and grain yield observed later in the field. Similar carry-over effects have been reported in rice and Arabidopsis, where early exposure to microbial or fungal VCs primes developmental and metabolic pathways that persist across growth stages [29,31,61] and sometime affects flowering time [62,63]. Thus, the improved yield and grain quality observed in both 2023 and 2024 may reflect an interaction between enhanced early vigor and favorable developmental timing rather than intrinsic HT stress tolerance alone.

WSFBs-derived VCs also increased tiller and panicle production, key determinants of sink capacity and yield potential [64–67]. These results align with reports that microbial signals, including VCs, modulate developmental pathways controlling tillering and biomass allocation [31,61,68]. The sustained increase in panicle number observed across both cultivars further indicates that WSFBs-VCs exposure positively influenced the key yield components.

Seed fertility remained stable or slightly improved in +VCs plants, even under the extreme HT of 2023. Spikelet sterility is a major constraint to rice productivity under HT conditions, particularly during the flowering stage [69–72]. The maintenance of fertility despite increased vegetative and reproductive sink development suggests that WSFBs-VCs treatment did not impose a reproductive trade-off. Instead, the combination of increased panicle number and stable fertility contributed to significant gains in total grain weight per plant, a widely recognized indicator of yield performance [73,74].

Grain appearance quality also improved following WSFBs-VCs exposure. +VCs plants produced a higher proportion of perfect grains and fewer severely chalky grains, particularly in the hotter season. Because chalkiness is closely associated with heat stress during grain filling [43,75], these results suggest that WSFB-derived VCs may help stabilize assimilate supply or endosperm development under elevated temperatures. Collectively, the field data demonstrate that seedling-stage exposure to WSFB-derived VCs enhances plant vigor, modifies developmental timing, and improves yield and grain quality under natural HT conditions.

Physiological and Molecular Responses Associated with WSFB-Derived VCs Under Acute Heat Stress

Gas-exchange measurements revealed that +VCs plants maintained higher net CO_2 assimilation, stomatal conductance, and intercellular CO_2 concentration under HT conditions. Because stomatal behavior is central to balancing CO_2 uptake and water loss [76–79], these responses provide a physiological basis for the improved growth and grain filling observed in the hot 2023 season. Although transpiration increased proportionally more than photosynthesis, resulting in reduced intrinsic water-use efficiency, this pattern is consistent with a shift toward transpirational cooling. Enhanced stomatal water flux can lower leaf and panicle temperatures, thereby sustaining photosynthesis during heat episodes [71,80–84]. This is a well-documented mechanism in heat-tolerant rice genotypes, whereby maintained higher stomatal conductance and cooler canopy temperatures during heat exposure is a key physiological basis for varietal HT tolerance in rice [83]. Thus, the observed decline in WUE likely reflects a heat-avoidance strategy rather than reduced physiological efficiency [77,84]. Nevertheless, these findings should be regarded as supportive physiological associations rather than definitive evidence of field-stage HT stress tolerance.

Controlled-HT environment assays provided mechanistic insight into molecular transcriptional responses associated with WSFBs-derived VCs. Under acute HT stress, +VCs seedlings maintained higher chlorophyll content, and lower malondialdehyde levels, indicating reduced oxidative damage and improved physiological stability responses commonly associated with heat tolerance [85,86]. Gene expression analyses further revealed that WSFBs-derived VCs modulated genes expression associated with cytokinine signaling and stress responses. Cytokinin-responsive regulators (*OsRR4, OsRR6, OsRR9, OsRR10*) were upregulated in +VCs treated seedlings and maintained the higher expression levels under HT stress. These type-A response regulators are rapidly inducible components of cytokinin signaling and influence shoot development, tillering, and stress adaptation [53,87–92]. Because active cytokinin plays an important role in axillary meristem activity, tiller formation, and grain development, the induction of these *OsRR* genes. It suggests that WSFBs-derived VCs may prime active cytokinin accumulation that contribute to improved vegetative development and stress adaptation. However, because cytokinin concentrations were not directly measured in this study, these findings should be interpreted as evidence of altered cytokinin-responsive signaling rather than direct confirmation of increased hormone levels. Genes involved in antioxidant and redox regulation, including *OsDHAR1*, *OsGRXS17*, and *OsGSTU6*, were also upregulated. These genes play central roles in the ascorbate-glutathione cycle and glutathione-dependent detoxification processes, which protect cells from oxidative damage during abiotic stress [93–98]. Dehydroascorbate reductase (DHAR) plays a central role in the ascorbate-glutathione cycle, a key antioxidant pathway that protects plant cells from oxidative damage by regenerating ascorbate and maintaining intracellular redox homeostasis [94,97]. Similarly, glutaredoxins (GRXs) and glutathione S-transferases (GSTs) regulate glutathione-dependent detoxification processes and contribute to cellular protection against oxidative stress during environmental challenges [95,96,98]. The increased expression of these genes in +VCs plants therefore suggests that WSFBs-derived VCs may likely enhance antioxidant defense capacity, enabling rice plants to mitigate oxidative damage generated under high-temperature stress. Additionally, the upregulation of *OsSNAC1* and *OsSLAC1*, key regulators of abiotic stress signaling and stomatal function [57,76,98–100], is consistent with the observed increases in photosynthetic activity, transpiration, and intercellular CO_2 concentration. Together, these molecular responses support the interpretation that WSFBs-derived VCs activate a coordinated network of hormonal, redox, and stress-responsive pathways that contribute to improved physiological performance under HT conditions.

Integrated Interpretation and Implications for Biostimulant Use

Taken together, the field, physiological, and transcriptional results indicate that WSFBs-derived VCs influence rice development through multiple interacting processes. Enhanced early vigor likely promotes stronger establishment and greater tiller formation, while shifts in flowering time may reduce exposure of reproductive stages to extreme heat. Concurrently, physiological adjustments, such as increased stomatal conductance, higher CO_2 assimilation, and improved oxidative stress protection, may help maintain plant function during heat episodes. These combined effects provide a coherent explanation for the improved yield and grain quality observed in +VCs plants.

From an agronomic perspective, the ability of a short seedling-stage treatment to enhance tiller formation, panicle number, grain yield, and grain quality is particularly promising. Microbial and fungal VCs are increasingly recognized as sustainable tools for crop improvement [27,37–39]. Using waste mushroom fungi beds substrates as a source of beneficial VCs aligns with circular bioeconomy principles and offers a low-cost, renewable biostimulant strategy for climate-resilient rice production.

Limitations and Future Work

Several limitations should be considered. First, volatile emissions were not quantified during the experiments. Although previous analyses of WSFBs identified bioactive compounds such as 3-octanone, 3-octanol, and 1-octen-3-one [40], future work should quantify emissions during exposure and establish dose,response relationships. Second, the controlled HT assay used acute seedling-stage stress (45/38 °C), whereas field plants experienced prolonged but less extreme temperatures. Because heat responses vary across developmental stages, the transcriptional responses observed in seedlings should be interpreted as mechanistic indicators rather than direct explanations for field outcomes. Third, field trials were conducted at a single site with modest sample sizes. Multi-location, larger-scale trials and additional rice genotypes will be necessary to assess broader applicability. Gas-exchange measurements were also taken at a single time point, limiting inference about temporal dynamics. Finally, transcriptional analyses were conducted only in Nipponbare; responses may differ in Koshihikari or other cultivars.

5. Conclusions

This study demonstrates that short-term exposure of rice seedlings to VCs emitted from WSFBs can generate lasting benefits that extend well beyond the seedling stage. Across two contrasting field seasons, including the record hot summer of 2023, WSFBs-derived VCs consistently enhanced early vigor, increased tiller and panicle production, advanced heading under high-temperature conditions, and improved both grain yield and appearance quality in two japonica cultivars. Controlled-environment assays further revealed that VCs exposure was associated with enhanced photosynthetic performance, improved redox and antioxidant regulation, and the induction of cytokinin- and stress-responsive genes during acute heat stress.

Together, these findings indicate that WSFB-derived VCs activate a coordinated set of developmental, physiological, and molecular responses that support improved plant performance under elevated temperatures. Importantly, the use of WSFBs—a readily available agricultural by-product, highlights a practical, low-cost, and circular bioeconomy approach for developing natural biostimulants. While further work is needed to validate performance across additional environments and cultivars, the present results provide strong evidence that WSFBs-derived VCs represent a promising strategy for enhancing rice resilience and productivity under future climate conditions.

Supplementary Materials: The following supporting information can be downloaded at the website of this paper posted on Preprints.org, Figure S1: Location of the paddy field experimental site at Shindori Station, Field Center for Sustainable Agriculture, Faculty of Agriculture, Niigata University, Niigata, Japan. Figure S2: Weather data and climate conditions during the 2023 and 2024 growing seasons. Figure S3: Classification of rice grain quality into perfect, moderately chalky, and severely chalky grains. Figure S4: Experimental workflow for field evaluation of rice seedlings exposed to WSFB-derived volatile compounds. Figure S5: Schematic overview of the controlled-environment experimental workflow for acute high-temperature stress treatment and sampling. Figure S6: Growth and physiological responses of Nipponbare rice seedlings exposed to WSFB-derived volatile compounds under acute high-temperature stress. Figure S7: Seedling vigor of Nipponbare and Koshihikari prior to paddy transplantation following exposure to WSFB-derived volatile compounds. Table S1: Experimental schedules for paddy field cultivation during the 2023 and 2024 growing seasons. Table S2: Heading dates of VC-treated and untreated rice plants across cultivars and growing seasons. Table S3: Micro-weather and seasonal temperature conditions during the 2023 and 2024 field experiments. Table S4: Growth and physiological traits of Nipponbare rice seedlings after 24 h of acute high-temperature stress. Table S5: Seedling vigor parameters of Nipponbare and Koshihikari prior to transplantation following exposure to WSFB-derived volatile compounds. Table S6: Primer sequences used for qPCR analysis.

Author Contributions: Conceptualization, C.N.K. and I.K.; methodology, C.N.K., S.R.S., and I.K.; investigation, C.N.K. and R.U.; formal analysis, C.N.K. and H.T.; data curation, C.N.K. and H.T.; validation, C.N.K. and I.K.; visualization, C.N.K.; writing original draft preparation, C.N.K.; writing, reviewing and editing, S.R.S., H.T., and I.K.; supervision, I.K. All authors have read and agreed to the published version of the manuscript.

Funding: This research was funded by the Japan Science and Technology Agency (JST), A-STEP Tryout, grant number JPMJTM22CA, and JST SPRING, grant number J3H2003.

Data Availability Statement: The data presented in this study are available on request from the corresponding author. The data are not publicly available because they form part of ongoing studies.

Acknowledgments: The authors are grateful to Niigata University for their support in providing research facilities. And we would like to thank Yairo Shiitake Buisness Cooperative and Hokken Co. Ltd for providing us with the waste shiitake fungi beds that were used in these studies.

Conflicts of Interest: The authors declare no conflicts of interest. The funders had no role in the design of the study; in the collection, analyses, or interpretation of data; in the writing of the manuscript; or in the decision to publish the results.

Abbreviations

The following abbreviations are used in this manuscript:

A_n	Net Photosynthetic Rate
Ci	Intercellular CO_2 Concentration
DHAR	Dehydroascorbate reductase
E	Transpiration Rate
FW	Fresh Weight
GRXs	glutaredoxins
GSTs	glutathione S-transferases
g_s	Stomatal Conductance
HS-SPME-GC-TOF/MS	Head Space Solid Phase Micro Extraction Gas Chromatography-Time of Flight-Mass Spectrometry
HISS	Heat-Induced Spikelet Sterility
HT	High temperature
HCA	Heatmap Clustering Analysis
MDA	Malondialdehyde
RRs	Response regulators
OTGW	One Thousand-Grain Weight
PBs	Plant biostimulants
PCA	Principal component analysis
PPFD	Photosynthetic photon flux density
PSII	photosystem II
qPCR	Quantitative Polymerase Chain Reaction
R	Statistical Software (R programming language)
ROS	Reactive oxygen species
SD	Standard deviation
TBA	Thiobarbituric Acid
TCA	Trichloroacetic Acid
VC	Volatile compound
VCs	Volatile compounds
WSFBs	Waste shiitake fungi beds
WUE	Water-Use Efficiency

References

1. Grigorieva, E.; Livenets, A.; Stelmakh, E. Adaptation of agriculture to climate change: A scoping review. *Climate* 2023, *11*, 202, doi:10.3390/cli11100202.
2. Seppelt, R.; Klotz, S.; Peiter, E.; Volk, M. Agriculture and food security under a changing climate: An underestimated challenge. *iScience* 2022, *25*, 105551, doi:10.1016/j.isci.2022.105551.
3. Smith, P.; Gregory, P.J. Climate change and sustainable food production. *Proc. Nutr. Soc.* **2013**, *72*, 21–28, doi:10.1017/S0029665112002832.
4. Hamadani, H.; Rashid, S.M.; Parrah, J.D.; Khan, A.A.; Dar, K.A.; Ganie, A.A.; Gazal, A.; Dar, R.A.; Ali, A. Traditional farming practices and its consequences. In *Microbiota and Biofertilizers, Vol 2: Ecofriendly Tools for Reclamation of Degraded Soil Environs*; Dar, G.H., Bhat, R.A., Mehmood, M.A., Hakeem, K.R., Eds.; Springer International Publishing: Cham, 2021; pp. 119–128 ISBN 978-3-030-61010-4, doi: 10.1007/978-3-030-61010-4_6
5. Kopecká, R.; Kameniarová, M.; Černý, M.; Brzobohatý, B.; Novák, J. Abiotic stress in crop production. *Int. J. Mol. Sci.* 2023, *24*, 6603, doi:10.3390/ijms24076603.
6. Kumar, R.; Lal, M.K.; Tiwari, R.K.; Kumar, A.; Behera, B.; Nayak, L.; Dash, G.K.; Sahoo, S.K.; Jena, J.; Lal, P.; et al. Traditional and emerging climate-resilient agricultural practices for enhancing food production and nutritional quality. In *New Frontiers in Plant-Environment Interactions: Innovative Technologies and Developments*; Aftab, T., Ed.; Springer Nature Switzerland: Cham, 2023; pp. 551–570 ISBN 978-3-031-43729-8, doi:10.1007/978-3-031-43729-8_21
7. Khalid, F.; Rasheed, Y.; Asif, K.; Ashraf, H.; Maqsood, M.F.; Shahbaz, M.; Zulfiqar, U.; Sardar, R.; Haider, F.U. Plant biostimulants: Mechanisms and applications for enhancing plant resilience to abiotic stresses. *J. Soil Sci. Plant Nutr.* 2024, *24*, 6641–6690, doi:10.1007/s42729-024-01996-3.
8. Di Sario, L.; Boeri, P.; Matus, J.T.; Pizzio, G.A. Plant biostimulants to enhance abiotic stress resilience in crops. *Int. J. Mol. Sci.* 2025, *26*, 1129, doi:10.3390/ijms26031129.
9. Rouphael, Y.; du Jardin, P.; Brown, P.; De Pascale, S.; Colla, G. Biostimulants for sustainable crop production; 2020; ISBN 978-1-78676-336-5, doi: 10.19103/AS.2020.0068
10. Yakhin, O.I.; Lubyanov, A.A.; Yakhin, I.A.; Brown, P.H. Biostimulants in plant science: A global perspective. *Front. Plant Sci.* 2017, *7*, doi:10.3389/fpls.2016.02049.
11. Mannino, G. Plant-biostimulants interaction: Scientific trends, markets dynamics, and real-world implication. *J. Plant Interact.* 2025, *20*, 2572668, doi:10.1080/17429145.2025.2572668.
12. Mannino, G. A New era of sustainability: Plant biostimulants. *Int. J. Mol. Sci.* 2023, *24*, 16329, doi:10.3390/ijms242216329.
13. Hijri, M. Microbial-based plant biostimulants. *Microorganisms* 2023, *11*, 686, doi:10.3390/microorganisms11030686.
14. Avalos, J.; Limón, M.C. Fungal secondary metabolism. *Encyclopedia* 2021, *2*, 1–13, doi:10.3390/encyclopedia2010001.
15. Bills, G.F.; Gloer, J.B. Biologically active secondary metabolites from the fungi. *Microbiol. Spectr.* 2016, *4*, 4.6.01, doi:10.1128/microbiolspec.FUNK-0009-2016.
16. Fukada, F. Mitigating the trade-off between growth and stress resistance in plants by fungal volatile compounds. *Plant Cell Physiol.* 2024, *65*, 175–178, doi:10.1093/pcp/pcae005.
17. Jampílek, J.; Kráľová, K. Fungal volatile organic compounds. In *Fungal Secondary Metabolites*; Elsevier, 2024; pp. 399–426 ISBN 978-0-323-95241-5, doi.org/10.1016/B978-0-323-95241-5.00016-2
18. Jiang, L.; Lee, M.H.; Kim, C.Y.; Kim, S.W.; Kim, P.I.; Min, S.R.; Lee, J. Plant growth promotion by two volatile organic compounds emitted from the fungus *Cladosporium Halotolerans* NGPF1. *Front. Plant Sci.* 2021, *12*, 794349, doi:10.3389/fpls.2021.794349.
19. Morath, S.U.; Hung, R.; Bennett, J.W. Fungal volatile organic compounds: A review with emphasis on their biotechnological potential. *Fungal Biol. Rev.* 2012, *26*, 73–83, doi:10.1016/j.fbr.2012.07.001.
20. Naik, B.S.; Rekha., D.; Deshpande, S.R. Volatile organic compounds from endophytic fungi and their role in plant growth and disease management. In *Fungal Endophytes Volume I: Biodiversity and Bioactive Materials*; Abd-Elsalam, K.A., AbuQamar, S.F., Eds.; Springer Nature: Singapore, 2025; pp. 241–259 ISBN 978-981-97-7312-1.

21. Lee, S.; Hung, R.; Bennett, J.W. An Overview of Fungal Volatile Organic Compounds (VOCs). In *Fungal Associations*; Hsueh, Y.-P., Blackwell, M., Eds.; Springer International Publishing: Cham, 2024; pp. 83–111 ISBN 978-3-031-41648-4, doi:10.1007/978-981-97-7312-1_9
22. Brosset, A.; Blande, J.D. Volatile-mediated plant–plant interactions: Volatile organic compounds as modulators of receiver plant defence, growth, and reproduction. *J. Exp. Bot.* 2022, *73*, 511–528, doi:10.1093/jxb/erab487.
23. El Jaddaoui, I.; Rangel, D.E.N.; Bennett, J.W. Fungal Volatiles Have Physiological Properties. *Fungal Biol.* 2023, *127*, 1231–1240, doi:10.1016/j.funbio.2023.03.005.
24. Minerdi, D.; Maggini, V.; Fani, R. Volatile organic compounds: From figurants to leading actors in fungal symbiosis. *FEMS Microbiol. Ecol.* 2021, *97*, fiab067, doi:10.1093/femsec/fiab067.
25. Hung, R.; Lee, S.; Bennett, J.W. Fungal Volatile organic compounds and their role in ecosystems. *Appl. Microbiol. Biotechnol.* 2015, *99*, 3395–3405, doi:10.1007/s00253-015-6494-4.
26. Farh, M.E.-A.; Jeon, J. Roles of fungal volatiles from perspective of distinct lifestyles in filamentous fungi. *Plant Pathol. J.* 2020, *36*, 193–203, doi:10.5423/PPJ.RW.02.2020.0025.
27. Fincheira, P.; Quiroz, A.; Tortella, G.; Diez, M.C.; Rubilar, O. Current advances in plant-microbe communication via volatile organic compounds as an innovative strategy to improve plant growth. *Microbiol. Res.* 2021, *247*, 126726, doi:10.1016/j.micres.2021.126726.
28. Jiménez-Bremont, J.F.; González-Pérez, E.; Ortega-Amaro, M.A.; Madrigal-Ortiz, S.; Duque-Ortiz, A.; Mendoza-Mendoza, A. Volatile organic compounds emitted by trichoderma: small molecules with biotechnological potential. *Sci. Hortic.* 2024, *325*, 112656, doi:10.1016/j.scienta.2023.112656.
29. Chiang, C.-Y.; Chang, C.-H.; Tseng, T.-Y.; Nguyen, V.-A.T.; Su, P.-Y.; Truong, T.-T.T.; Chen, J.-Y.; Huang, C.-C.; Huang, H.-J. Volatile compounds emitted by plant growth-promoting fungus *Tolypocladium Inflatum* GT22 alleviate copper and pathogen stress. *Plant Cell Physiol.* 2024, *65*, 199–215, doi:10.1093/pcp/pcad120.
30. Asghar, W.; Kataoka, R. Fungal volatiles from green manure-incorporated soils promote the growth of lettuce (*Lactuca Sativa*) and mediate antifungal activity against *Fusarium Oxysporum* in vitro. *Plant Soil* 2023, doi:10.1007/s11104-023-06158-5.
31. Chen, H.; Xu, J.; Shao, D.; Zhao, C.; Xu, X.; Xu, X.; Chen, C. Growth promotion of rice and *Arabidopsis Thaliana* by volatile organic compounds produced by endophytic *Clonostachys* species. *J. Fungi* 2024, *10*, 754, doi:10.3390/jof10110754.
32. Razo-Belmán, R.; Ángeles-López, Y.I.; García-Ortega, L.F.; León-Ramírez, C.G.; Ortiz-Castellanos, L.; Yu, H.; Martínez-Soto, D. Fungal volatile organic compounds: Mechanisms involved in their sensing and dynamic communication with plants. *Front. Plant Sci.* 2023, *14*, 1257098, doi:10.3389/fpls.2023.1257098.
33. Sánchez-López, Á.M.; Baslam, M.; De Diego, N.; Muñoz, F.J.; Bahaji, A.; Almagro, G.; Ricarte-Bermejo, A.; García-Gómez, P.; Li, J.; Humplík, J.F.; et al. Volatile compounds emitted by diverse phytopathogenic microorganisms promote plant growth and flowering through cytokinin action. *Plant Cell Environ.* 2016, *39*, 2592–2608, doi:10.1111/pce.12759.
34. Naik, H.; Chandarana, K.A.; Gamit, H.A.; Chandwani, S.; Amaresan, N. Microbial volatile compounds: Prospects for fungal phytopathogens management, mechanisms and challenges. *J. Crop Health* 2024, *76*, 371–383, doi:10.1007/s10343-023-00951-z.
35. Fadiji, A.E.; Babalola, O.O.; Santoyo, G.; Perazzolli, M. The potential role of microbial biostimulants in the amelioration of climate change-associated abiotic stresses on crops. *Front. Microbiol.* 2022, *12*, 829099, doi:10.3389/fmicb.2021.829099.
36. Phoka, N.; Suwannarach, N.; Lumyong, S.; Ito, S.; Matsui, K.; Arikit, S.; Sunpapao, A. Role of volatiles from the endophytic fungus *Trichoderma Asperelloides* PSU-P1 in biocontrol potential and in promoting the plant growth of *Arabidopsis Thaliana*. *J. Fungi* 2020, *6*, 341, doi:10.3390/jof6040341.
37. Garg, S.; Kim, M.; Romero-Suarez, D. Current advancements in fungal engineering technologies for sustainable development goals. *Trends Microbiol.* 2025, *33*, 285–301, doi:10.1016/j.tim.2024.11.001.
38. Lange, L.; Agger, J.W.; Meyer, A.S. Fungal biotechnology: Unlocking the full potential of fungi for a more sustainable world. In *Grand Challenges in Fungal Biotechnology*; Nevalainen, H., Ed.; Springer International Publishing: Cham, 2020; pp. 3–32 ISBN 978-3-030-29541-7, doi:10.1007/978-3-030-29541-7_1

39. Meyer, V.; Cairns, T.; Barthel, L.; King, R.; Kunz, P.; Schmideder, S.; Müller, H.; Briesen, H.; Dinius, A.; Krull, R. Understanding and controlling filamentous growth of fungal cell factories: Novel tools and opportunities for targeted morphology engineering. *Fungal Biol. Biotechnol.* 2021, *8*, 8, doi:10.1186/s40694-021-00115-6.
40. Kanga, C.N.; Okisaka, Y.; Hanamata, S.; Ueda, D.; Sato, T.; Mitsui, T.; Itoh, K. Development of an application method for volatile compounds derived from mushroom fungi beds as plant growth-promoting biostimulants. *Methods Protoc.* 2025, *8*, 29, doi:10.3390/mps8020029.
41. Sayre, L.B. The pre-history of soil science: Jethro Tull, the invention of the seed drill, and the foundations of modern agriculture. *Phys. Chem. Earth Parts ABC* 2010, *35*, 851–859, doi:10.1016/j.pce.2010.07.034.
42. Singh, S.; Bargali, S.; Patel, J.; Singh, R. Technique of rice (*Oryza Sativa*) seed selection in salt solution-an evaluation under real farm situation. 2007, *25*, 461–463.
43. Ishfaq, J.; Soomar, A.M.; Khalid, F.; Abbasi, Y. Assessing rice (*Oryza Sativa* L.) quality: A comprehensive review of current techniques and future directions. *J. Agric. Food Res.* 2023, *14*, 100843, doi:10.1016/j.jafr.2023.100843.
44. Mathan, J.; Singh, A.; Jathar, V.; Ranjan, A. High photosynthesis rate in two wild rice species is driven by leaf anatomy mediating high rubisco activity and electron transport rate. *J. Exp. Bot.* 2021, *72*, 7119–7135, doi:10.1093/jxb/erab313.
45. Savvides, A.M.; Fotopoulos, V. Two inexpensive and non-destructive techniques to correct for smaller-than-gasket leaf area in gas exchange measurements. *Front. Plant Sci.* 2018, *9*, 548, doi:10.3389/fpls.2018.00548.
46. Sarker, M.H.; Hussain, M.H.; Neik, T.X.; Hasan, M.Z.; Wee, W.Y.; Tan, H.S.; Ko, S.; Song, B.-K. Screening of Heat stress-tolerant weedy rice and SNP identification of heat-tolerance-related genes. *Plant Biotechnol. Rep.* 2024, *18*, 659–672, doi:10.1007/s11816-024-00920-6.
47. Xing, Y.-H.; Lu, H.; Zhu, X.; Deng, Y.; Xie, Y.; Luo, Q.; Yu, J. How rice responds to temperature changes and defeats heat stress. *Rice* 2024, *17*, 73, doi:10.1186/s12284-024-00748-2.
48. He, Y.; Guan, H.; Li, B.; Zhang, S.; Xu, Y.; Yao, Y.; Yang, X.; Zha, Z.; Guo, Y.; Jiao, C.; et al. Transcriptome analysis reveals the dynamic and rapid transcriptional reprogramming involved in heat stress and identification of heat response genes in rice. *Int. J. Mol. Sci.* 2023, *24*, 14802, doi:10.3390/ijms241914802.
49. Senthilkumar, M.; Amaresan, N.; Sankaranarayanan, A. Estimation of malondialdehyde (MDA) by Thiobarbituric acid (TBA) assay. In *Plant-Microbe Interactions: Laboratory Techniques*; Senthilkumar, M., Amaresan, N., Sankaranarayanan, A., Eds.; Springer US: New York, NY, 2021; pp. 103–105 ISBN 978-1-0716-1080-0, doi:10.1007/978-1-0716-1080-0_25
50. LICHTENTHALER, H.K.; WELLBURN, A.R. Determinations of Total Carotenoids and Chlorophylls a and b of Leaf Extracts in Different Solvents. *Biochem. Soc. Trans.* 1983, *11*, 591–592, doi:10.1042/bst0110591.
51. Su, S.; Zhou, Y.; Qin, J.G.; Yao, W.; Ma, Z. Optimization of the method for chlorophyll extraction in aquatic plants. *J. Freshw. Ecol.* 2010, *25*, 531–538, doi:10.1080/02705060.2010.9664402.
52. Livak, K.J.; Schmittgen, T.D. Analysis of relative gene expression data using Real-Time Quantitative PCR and the 2−ΔΔCT method. *Methods* 2001, *25*, 402–408, doi:10.1006/meth.2001.1262.
53. Jain, M.; Tyagi, A.K.; Khurana, J.P. Molecular characterization and differential expression of cytokinin-responsive Type-A response regulators in rice (*Oryza Sativa*). *BMC Plant Biol.* 2006, *6*, 1, doi:10.1186/1471-2229-6-1.
54. Saha, S.R.; Islam, S.M.S.; Itoh, K. Identification of abiotic stress-responsive genes: A genome-wide analysis of the cytokinin response regulator gene family in rice. *Genes Genet. Syst.* 2024, *99*, doi:10.1266/ggs.24-00068.
55. Jing, X.-Q.; Zhou, M.-R.; Nie, X.-M.; Zhang, L.; Shi, P.-T.; Shalmani, A.; Miao, H.; Li, W.-Q.; Liu, W.-T.; Chen, K.-M. *OsGSTU6* contributes to cadmium stress tolerance in rice by involving in intracellular ROS homeostasis. *J. Plant Growth Regul.* 2021, *40*, 945–961, doi:10.1007/s00344-020-10148-7.
56. Hu, Y.; Wu, Q.; Peng, Z.; Sprague, S.A.; Wang, W.; Park, J.; Akhunov, E.; Jagadish, K.S.V.; Nakata, P.A.; Cheng, N.; et al. Silencing of *OsGRXS17* in rice improves drought stress tolerance by modulating ROS accumulation and stomatal closure. *Sci. Rep.* 2017, *7*, 15950, doi:10.1038/s41598-017-16230-7.

57. Sun, S.-J.; Qi, G.-N.; Gao, Q.-F.; Wang, H.-Q.; Yao, F.-Y.; Hussain, J.; Wang, Y.-F. Protein kinase *OsSAPK8* functions as an essential activator of S-Type anion channel *OsSLAC1*, which is Nitrate-selective in rice. *Planta* 2016, *243*, 489–500, doi:10.1007/s00425-015-2418-x.
58. Do, H.; Kim, I.-S.; Jeon, B.W.; Lee, C.W.; Park, A.K.; Wi, A.R.; Shin, S.C.; Park, H.; Kim, Y.-S.; Yoon, H.-S.; et al. Structural understanding of the recycling of oxidized ascorbate by Dehydroascorbate reductase (*OsDHAR*) from *Oryza Sativa* L. *Japonica*. *Sci. Rep.* 2016, *6*, 19498, doi:10.1038/srep19498.
59. Qi, J.; Yu , L.; Ding, J.; Ji, C.; Wang, S.; Wang, C.; Ding, G.; Shi, L.; Xu, F.; Cai, H. Transcription factor *OsSNAC1* positively regulates nitrate transporter gene expression in rice. *Plant Physiol.* 2023, *192*, 2923–2942, doi:10.1093/plphys/kiad290.
60. Li, X.; Chang, Y.; Ma, S.; Shen, J.; Hu, H.; Xiong, L. Genome-wide identification of *SNAC1*-targeted genes involved in drought response in rice. *Front. Plant Sci.* 2019, *10*, 982, doi:10.3389/fpls.2019.00982.
61. Almeida, O.A.C.; de Araujo, N.O.; Mulato, A.T.N.; Persinoti, G.F.; Sforça, M.L.; Calderan-Rodrigues, M.J.; Oliveira, J.V. de C. Bacterial volatile organic compounds (VOCs) promote growth and induce metabolic changes in rice. *Front. Plant Sci.* 2023, *13*, doi:10.3389/fpls.2022.1056082.
62. Kazan, K.; Lyons, R. The link between flowering time and stress tolerance. *J. Exp. Bot.* **2016**, *67*, 47–60, doi:10.1093/jxb/erv441.
63. Tan, B.C.; Lau, S.-E.; Lim, L.W.T.; Hamdan, M.F.; Chan, C.; Saidi, N.B.; Ong-Abdullah, J. Enhancing plant resilience to abiotic stress: The power of biostimulants. *Phyton* 2025, *94*, 1–31, doi:10.32604/phyton.2025.059930.
64. Martinez-Eixarch, M.; Català, M.D.M.; Tomàs, N.; Pla, E.; Zhu, D. Tillering and yield formation of a temperate japonica rice cultivar in a mediterranean rice agrosystem. *Span. J. Agric. Res.* 2015, *13*, e0905, doi:10.5424/sjar/2015134-7085.
65. Takai, T. Potential of rice tillering for sustainable food production. *J. Exp. Bot.* 2024, *75*, 708–720, doi:10.1093/jxb/erad422.
66. Zhang, N.; Liu, Y.; Gui, S.; Wang, Y. Regulation of tillering and panicle branching in rice and wheat. *J. Genet. Genomics* 2025, *52*, 869–886, doi:10.1016/j.jgg.2024.12.005.
67. Sloan, J.M.; Mujab, A.A.M.; Mashitah, J.; Zulkarami, B.; Wilson, M.J.; Toh, L.S.; Nur Zahirah, A.J.; Afiq, K.; Asyraf, A.T.; Zhu, X.-G.; et al. Elevated CO_2 priming as a sustainable approach to increasing rice tiller number and yield potential. *Rice* 2023, *16*, 16, doi:10.1186/s12284-023-00629-0.
68. Zhang, J.; Wang, B.; Xu, H.; Liu, W.; Yu, J.; Wang, Q.; Yu, H.; Wei, J.-W.; Dai, R.; Zhou, J.; et al. Root microbiota regulates tiller number in rice. *Cell* 2025, *188*, 3152-3166.e16, doi:10.1016/j.cell.2025.03.033.
69. Hasegawa, T.; Ishimaru, T.; Kondo, M.; Kuwagata, T.; Yoshimoto, M.; Fukuoka, M. Spikelet sterility of rice observed in the record hot summer of 2007 and the factors associated with its variation. *J. Agric. Meteorol.* 2011, *67*, 225–232, doi:10.2480/agrmet.67.4.3.
70. Matsui, T. Floret sterility induced by high temperatures at the flowering stage in rice (*Oryza Sativa* L.). *Jpn. J. Crop Sci.* 2009, *78*, 303–311, doi:10.1626/jcs.78.303.
71. Yoshimoto, M.; Sakai, H.; Ishigooka, Y.; Kuwagata, T.; Ishimaru, T.; Nakagawa, H.; Maruyama, A.; Ogiwara, H.; Nagata, K. Field survey on rice spikelet sterility in an extremely hot summer of 2018 in japan. *Agric. Met*. 2021, *77*, 262–269, doi:10.2480/agrmet.D-21-00024.
72. Satake, T.; Yoshida, S. High temperature-induced sterility in indica rices at flowering. *Jpn. J. Crop Sci.* 1978, *47*, 6–17, doi:10.1626/jcs.47.6.
73. Chen, K.; Łyskowski, A.; Jaremko, Ł.; Jaremko, M. Genetic and molecular factors determining grain weight in rice. *Front. Plant Sci.* 2021, *12*, 605799, doi:10.3389/fpls.2021.605799.
74. Saito, H.; Fukuta, Y.; Obara, M.; Tomita, A.; Ishimaru, T.; Sasaki, K.; Fujita, D.; Kobayashi, N. Two novel QTLs for the harvest index that contribute to high-yield production in rice (*Oryza Sativa* L.). *Rice* 2021, *14*, 18, doi:10.1186/s12284-021-00456-1.
75. Tsukaguchi, T.; Iida, Y. Effects of assimilate supply and high temperature during grain-filling period on the occurrence of various types of chalky kernels in rice plants (*Oryza Sativa* L.). *Plant Prod. Sci.* 2008, *11*, 203–210, doi:10.1626/pps.11.203.
76. Hedrich, R.; Geiger, D. Biology of SLAC1-Type anion channels - from nutrient uptake to stomatal closure. *New Phytol.* 2017, *216*, 46–61, doi:10.1111/nph.14685.

77. Wang, Z.; Slot, M.; Wang, C. Decoupling of stomatal conductance, transpiration and photosynthesis in terrestrial plants under elevated temperature: A meta-analysis. *Nat. Commun.* 2026, *17*, 1528, doi:10.1038/s41467-025-68250-x.
78. Ouyang, W.; Struik, P.C.; Yin, X.; Yang, J. Stomatal conductance, mesophyll conductance, and transpiration efficiency in relation to leaf anatomy in rice and wheat genotypes under drought. *J. Exp. Bot.* 2017, *68*, 5191–5205. doi:10.1093/jxb/erx314.
79. Malini, M.K.; Karwa, S.; Priyadarsini, P.; Kumar, P.; Nagar, S.; Kumar, M.; Kumar, S.; Chinnusamy, V.; Pandey, R.; Pal, M. Abscisic-acid-modulated stomatal conductance governs high-temperature stress tolerance in rice accessions. *Agriculture* 2023, *13*, 545, doi:10.3390/agriculture13030545.
80. Lawson, T.; Vialet-Chabrand, S. Speedy stomata, photosynthesis and plant water use efficiency. *New Phytol.* 2019, *221*, 93–98, doi:10.1111/nph.15330.
81. Rathnasamy, S.A.; Kambale, R.; Elangovan, A.; Mohanavel, W.; Shanmugavel, P.; Ramasamy, G.; Alagarsamy, S.; Marimuthu, R.; Rajagopalan, V.R.; Manickam, S.; et al. Altering stomatal density for manipulating transpiration and photosynthetic traits in rice through CRISPR/Cas9 mutagenesis. *Curr. Issues Mol. Biol.* 2023, *45*, 3801–3814, doi:10.3390/cimb45050245.
82. Mu, Q.; Wang, S.; Liu, Y.; Gao, Y.; Liu, W.; Okpala, N.E. Transpirational cooling enhances grain yield and quality in heat-tolerant rice varieties. *Front. Plant Sci.* 2025, *16*, doi:10.3389/fpls.2025.1660130.
83. Yin, Q.; Tian, T.; Kou, M.; Liu, P.; Wang, L.; Hao, Z.; Yue, M. The relationships between photosynthesis and stomatal traits on the loess plateau. *Glob. Ecol. Conserv.* 2020, *23*, e01146, doi:10.1016/j.gecco.2020.e01146.
84. Hatfield, J.L.; Dold, C. Water-use efficiency: Advances and challenges in a changing climate. *Front. Plant Sci.* **2019**, *10*, doi:10.3389/fpls.2019.00103.
85. Huang, S.; Deng, Q.; Zhao, Y.; Chen, G.; Geng, A.; Wang, X. L -Glutamate seed priming enhances 2-Acetyl-1-pyrroline formation in fragrant rice seedlings in response to arsenite stress. *J. Agric. Food Chem.* 2023, *71*, 18443–18453, doi:10.1021/acs.jafc.3c06369.
86. Jahan, M.S.; Hasan, M.M.; Rahman, M.A. Editorial: Hormones and biostimulants in plants: Physiological and molecular insights on plant stress responses. *Front. Plant Sci.* 2024, *15*, 1413659, doi:10.3389/fpls.2024.1413659.
87. Ashikari, M.; Sakakibara, H.; Lin, S.; Yamamoto, T.; Takashi, T.; Nishimura, A.; Angeles, E.R.; Qian, Q.; Kitano, H.; Matsuoka, M. Cytokinin oxidase regulates rice grain production. *Science* 2005, *309*, 741–745, doi:10.1126/science.1113373.
88. Bhaskar, A.; Paul, L.K.; Sharma, E.; Jha, S.; Jain, M.; Khurana, J.P. *OsRR6*, a Type-A response regulator in rice, mediates cytokinin, light and stress responses when over-expressed in *Arabidopsis*. *Plant Physiol. Biochem.* 2021, *161*, 98–112, doi:10.1016/j.plaphy.2021.01.047.
89. Panda, B.B.; Sekhar, S.; Dash, S.K.; Behera, L.; Shaw, B.P. Biochemical and molecular characterisation of exogenous cytokinin application on grain filling in rice. *BMC Plant Biol.* 2018, *18*, 89, doi:10.1186/s12870-018-1279-4.
90. Liu, B.; Meng, S.; Yang, J.; Wu, J.; Peng, Y.; Zhang, J.; Ye, N. Carbohydrate flow during grain filling: Phytohormonal regulation and genetic control in rice (*Oryza Sativa*). *J. Integr. Plant Biol.* 2025, *67*, 1086–1104, doi:10.1111/jipb.13904.
91. Li, M.; Feng, L.; Ye, H.; Li, M.; Jin, J.; Tao, L.-Z.; Liu, H. *OsRopGEF10* attenuates cytokinin signaling to regulate panicle development and grain yield in rice. *Rice* 2024, *17*, 57, doi:10.1186/s12284-024-00737-5.
92. Hirose, N.; Makita, N.; Kojima, M.; Kamada-Nobusada, T.; Sakakibara, H. Overexpression of a Type-A response regulator alters rice morphology and cytokinin metabolism. *Plant Cell Physiol.* 2007, *48*, 523–539, doi:10.1093/pcp/pcm022.
93. Kim, Y.-S.; Park, S.-I.; Kim, J.-J.; Shin, S.-Y.; Kwak, S.-S.; Lee, C.-H.; Park, H.-M.; Kim, Y.-H.; Kim, I.-S.; Yoon, H.-S. Over-expression of Dehydroascorbate Reductase improves salt tolerance, environmental adaptability and productivity in *Oryza Sativa*. *Antioxid. Basel Switz.* 2022, *11*, 1077, doi:10.3390/antiox11061077.
94. Foyer, C.H.; Noctor, G. Ascorbate and Glutathione: The heart of the Redox hub. *Plant Physiol.* 2011, *155*, 2-18, doi:10.1104/pp.110.167569.

95. Martins, L.; Knuesting, J.; Bariat, L.; Dard, A.; Freibert, S.A.; Marchand, C.H.; Young, D.; Dung, N.H.T.; Voth, W.; Debures, A.; et al. Redox modification of the Iron-Sulfur Glutaredoxin GRXS17 activates Holdase activity and protects plants from heat stress. *Plant Physiol.* 2020, *184*, 676–692, doi:10.1104/pp.20.00906.
96. Zhai, R.; Ye, S.; Ye, J.; Wu, M.; Zhu, G.; Yu, F.; Wang, X.; Feng, Y.; Zhang, X. Glutaredoxin in rice growth, development, and stress resistance: Mechanisms and research advances. *Int. J. Mol. Sci.* 2023, *24*, 16968, doi:10.3390/ijms242316968.
97. Jing, X.-Q.; Zhou, M.-R.; Nie, X.-M.; Zhang, L.; Shi, P.-T.; Shalmani, A.; Miao, H.; Li, W.-Q.; Liu, W.-T.; Chen, K.-M. *OsGSTU6* contributes to cadmium stress tolerance in rice by involving in intracellular ROS homeostasis. *J. Plant Growth Regul.* 2021, *40*, 945–961, doi:10.1007/s00344-020-10148-7.
98. Kurowska, M.; Daszkowska-Golec, A. Molecular mechanisms of SNAC1 (Stress-Responsive NAC1) in conferring the abiotic stress tolerance. *Plant Sci.* 2023, *337*, 111894, doi:10.1016/j.plantsci.2023.111894.
99. Kusumi, K.; Hirotsuka, S.; Kumamaru, T.; Iba, K. increased leaf photosynthesis caused by elevated stomatal conductance in a rice mutant deficient in *SLAC1*, a guard cell anion channel protein. *J. Exp. Bot.* 2012, *63*, 5635–5644, doi:10.1093/jxb/ers216.
100. You, J.; Zong, W.; Li, X.; Ning, J.; Hu, H.; Li, X.; Xiao, J.; Xiong, L. The SNAC1-targeted gene *OsSRO1c* modulates stomatal closure and oxidative stress tolerance by regulating hydrogen peroxide in rice. *J. Exp. Bot.* 2013, *64*, 569–583, doi:10.1093/jxb/ers349.